

Supplementary Information

Highly fluorescent complexes with 3-isocyanoperylene and *N*-(2,5-di-tert-butylphenyl)-9-isocyanoperylene-3,4-dicarboximide

Sergio Lentijo,[†] J. Emilio Expósito,[†] Gabriel Aullón,[‡] Jesús A. Miguel,^{†,*} and Pablo Espinet.^{†,*}

IU CINQUIMA Química Inorgánica, Facultad de Ciencias, Universidad de Valladolid, E-47071 Valladolid, Spain; and Departament de Química Inorgànica, Universitat de Barcelona, Martí i Franquès 1-11, E-08028 Barcelona, Spain.

Fig. S1 Absorption spectra of PMI-NC and their complexes **5a**, **9a-12a**, recorded in CHCl₃ solution ($\sim 10^{-5}$ M) at room temperature

Fig. S2 Absorption spectra of Per-NC and their complexes **5b-11b**, recorded in CHCl₃ solution ($\sim 10^{-5}$ M) at room temperature

Fig. S3 Emission spectra of **11b** in different solvents (ca. 10^{-5} M) at room temperature.

Fig. S4 Schematic representation of main expected transition in the absorption spectra of PMIH and perylene.

Table S1 Calculated absorption parameters (wavelengths in nm and their intensities) for R-X (R = PMI and Per) compounds in gas phase and chloroform solution.

Table S2 Calculated absorption peaks for [M(CO)₅(CNR)] (M = Cr, Mo, W; R = PMI, Per).

Fig. S5 ¹H and ¹⁹F NMR spectra

Fig. S6 IR spectra

Fig. S7 Fluorescence decays in dichloromethane, at room temperature

[†] Universidad de Valladolid

[‡] Universitat de Barcelona

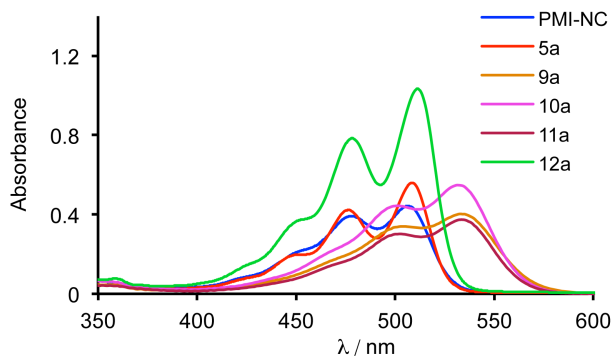


Figure S1. Absorption spectra of PMI-NC and their complexes **5a**, **9a-12a**, recorded in CHCl_3 solution ($\sim 10^{-5}$ M) at room temperature

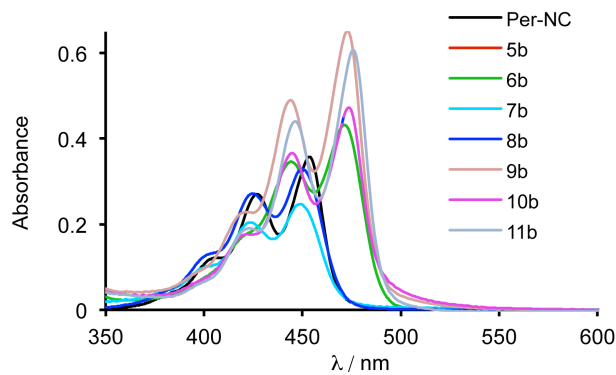


Figure S2. Absorption spectra of Per-NC and their complexes **5b-11b**, recorded in CHCl_3 solution ($\sim 10^{-5}$ M) at room temperature

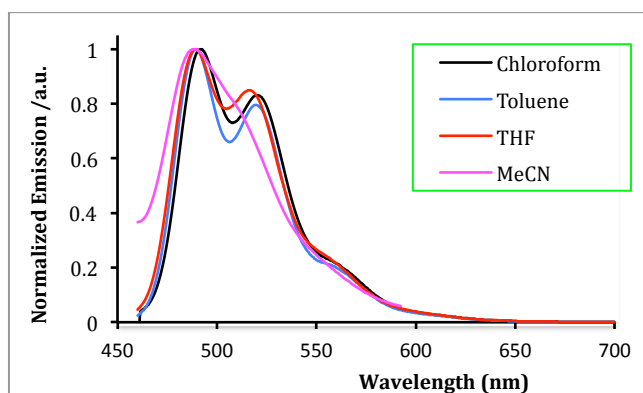


Fig. S3 Emission spectra of **11b** in different solvents (ca. 10^{-5} M) at room temperature.

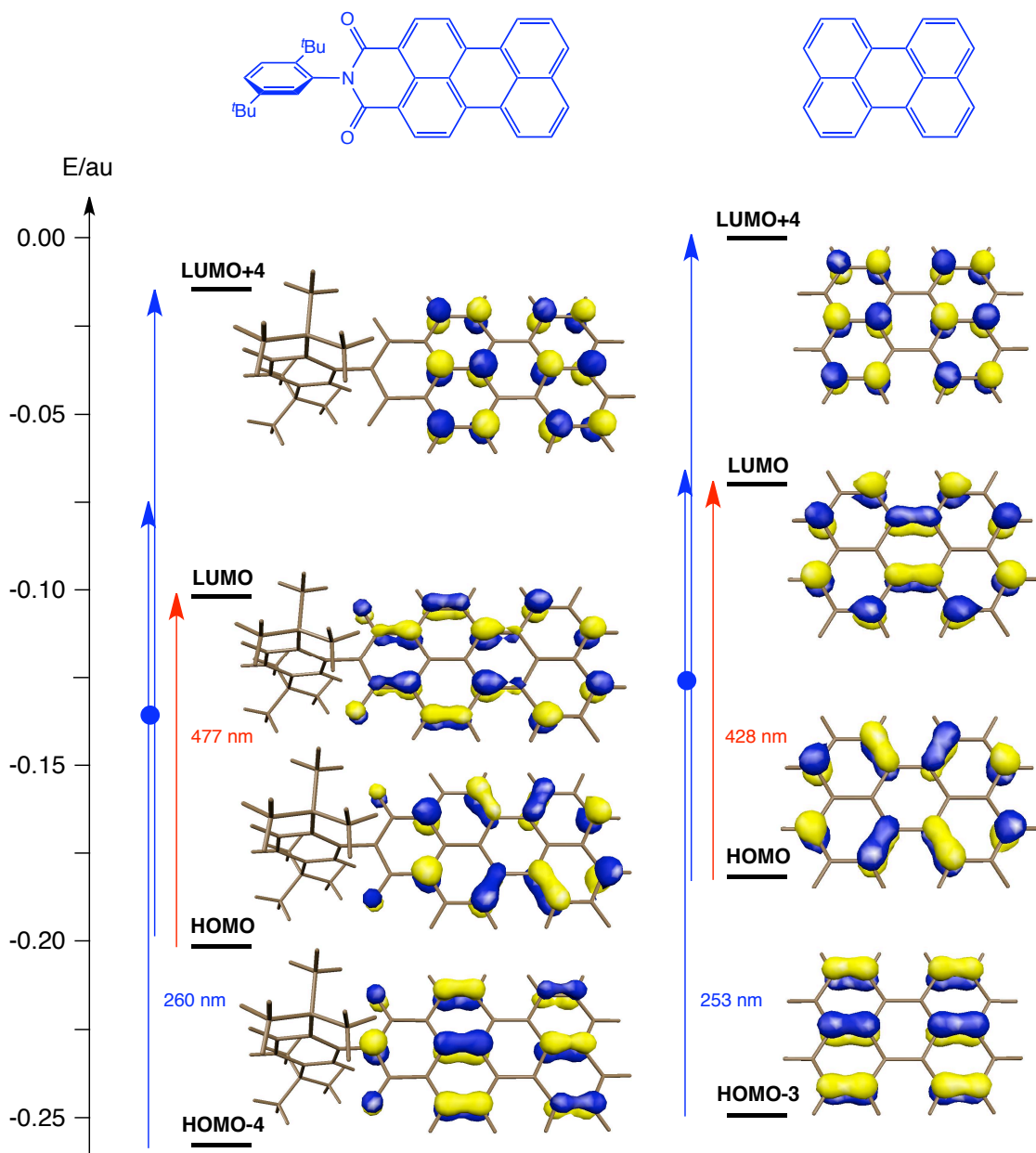


Fig. S4 Schematic representation of main expected transition in the absorption spectra of PMIH and perylene.

Table S1. Calculated absorption parameters (wavelengths in nm, oscillator strength (f), and coefficients of the main contributions of the orbitals [in brackets]) for R-X (R = PMI and Per) compounds in gas phase and chloroform solution.

(a) Organics

λ (f)	Solvent	H	NC
PMI-X	Gas phase	477 (0.61) [0.62]	490 (0.69) [0.61]
		260 (0.09), 259 (0.11) [0.48, 0.38],[0.44,0.40]	261 (0.19) [0.55,0.23]
	CHCl_3	500 (0.77) [0.63]	512 (0.86) [0.63]
		262 (0.26) [0.55,0.15]	263 (0.22) [0.51,0.30]
Per-X	Gas phase	428 (0.36) [0.62]	446 (0.44) [0.62]
		253 (0.30) [0.48,0.36]	257 (0.28) [0.48,0.25]
	CHCl_3	442 (0.48) [0.63]	465 (0.58) [0.63]
		257 (0.51) [0.50,0.38]	260 (0.44) [0.51,0.22]

^a Coefficients are $[\pi_{HOMO} \rightarrow \pi^*_{LUMO}]$ for first transition in all cases, and $[\pi_{HOMO} \rightarrow \pi^*, \pi \rightarrow \pi^*_{LUMO}]$ for second band of perylene systems.

(b) Chromium complexes

$\lambda (f)$	$[(PMI-NC)Cr(CO)_5]$	$[(PerNC)Cr(CO)_5]$
Gas phase	518 (0.97)	468 (0.70)
	$\pi(PMI)_H \rightarrow \pi^*(PMI-NC)_L$ [0.70]	$\pi(Per)_H \rightarrow \pi^*(Per-NC)_L$ [0.70]
	281 (0.08)	259 (0.15)
	$\pi(CO) + \pi d \rightarrow \pi^*(CO)_{eq}$ [0.52]	$\pi(Per)_H \rightarrow \pi^*(Per)$ [0.42]
	$\pi(CO) \rightarrow \pi^*(PMI-NC)$ [0.33]	$\pi d \rightarrow \pi^*(Per)$ [0.26]
	266 (0.09)	
	$\pi(CO) + \pi d \rightarrow \pi^*(PMI-NC)$ [0.54]	
	$\pi(PMI) \rightarrow \pi^*(PMI)$ [0.24]	
	536 (1.14)	482 (0.84)
	$\pi(PMI)_H \rightarrow \pi^*(PMI-NC)_L$ [0.70]	$\pi(Per)_H \rightarrow \pi^*(Per-NC)_L$ [0.70]
$CHCl_3$	282 (0.10)	265 (0.19)
	$\pi(CO) + \pi d \rightarrow \pi^*(CO)_{eq}$ [0.54]	$\pi(Per)_H \rightarrow \pi^*(Per)$ [0.35]
	$\pi(CO) + \pi d \rightarrow \pi^*(PMI-NC)$ [0.31]	$\pi d \rightarrow \pi^*(CO)_{eq}$ [0.31]
	264 (0.12)	$\pi d \rightarrow \pi^*(CO)_{eq}$ [0.24]
	$\pi(PMI) \rightarrow \pi^*(PMI)$ [0.38]	262 (0.22)
	$\pi(CO) + \pi d \rightarrow \pi^*(CO)_{eq}$ [0.35]	$\pi(Per)_H \rightarrow \pi^*(Per)$ [0.37]
		$\pi d \rightarrow \pi^*(CO)_{eq}$ [0.28]
		$\pi d \rightarrow \pi^*(NC)$ [0.23]

Annotation for the involved orbitals:

- $\pi(PMI)$ and $\pi(Per)$ indicate generic occupied orbitals as well as $\pi^*(PMI)$, and $\pi^*(Per)$ are empty ones. Since all of these orbitals are of type π , only H and L are emphasized. Orbital contribution on the nitrile group included when remarkable.
- $\pi(Ph)$ and $\pi^*(Ph)$ are occupied and empty orbitals centered in the phenylic diimido substituent.
- Other fragments such as C_6F_5 or CO are also used to designate centered π orbitals.
- Other d -orbitals are generally written as πd .

(c) Gold complexes

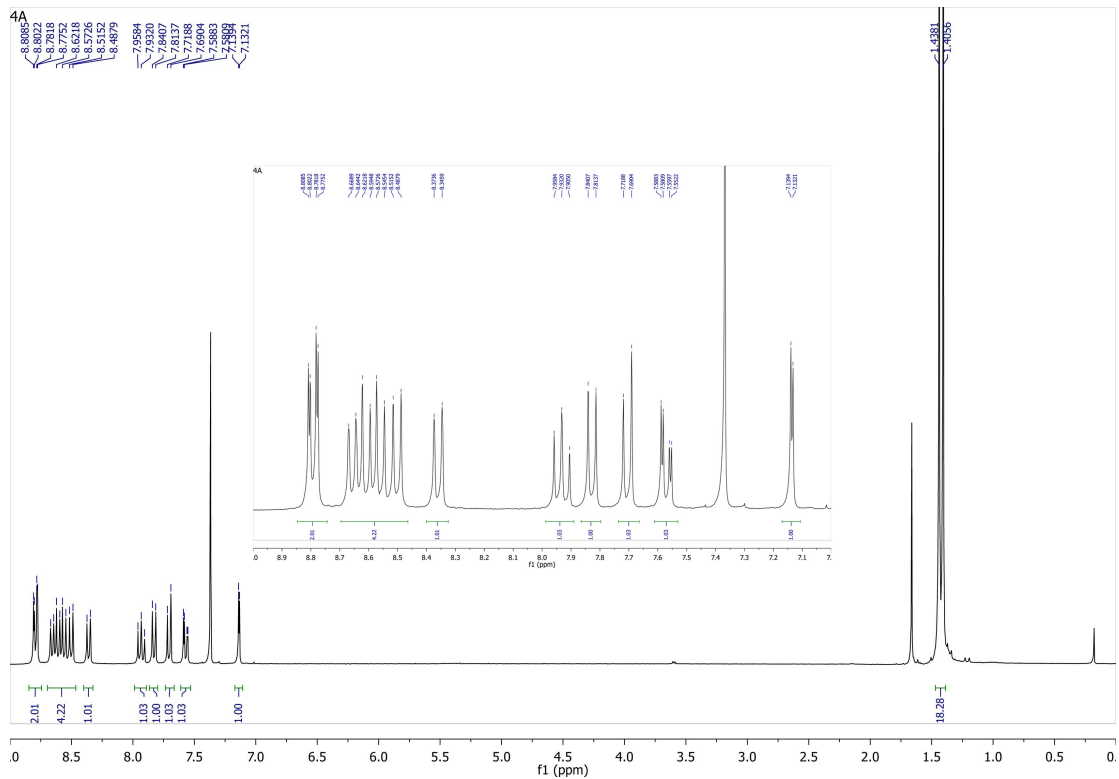
λ (f)	[(PMI-NC)Au(C ₆ F ₅)]	[(PerNC)Au(C ₆ F ₅)]
Gas phase	519 (0.79)	474 (0.69)
	$\pi(PMI)_H \rightarrow \pi^*(PMI-NC)_L$ [0.68]	$\pi(Per)_H \rightarrow \pi^*(Per-NC)_L$ [0.70]
	481 (0.15)	296 (0.25)
	$\pi(C_6F_5) \rightarrow \pi^*(PMI-NC)_L$ [0.64]	$\pi(C_6F_5) \rightarrow \pi^*(Per-NC)$ [0.53]
	325 (0.12)	262 (0.19)
	$\pi(C_6F_5) \rightarrow \pi^*(PMI-NC)$ [0.63]	$\pi(Per)_H \rightarrow \pi^*(Per-NC)$ [0.49]
	269 (0.10)	$\pi(Per) \rightarrow \pi^*(Per-NC)_L$ [0.26]
	$\pi(PMI)_H \rightarrow \pi^*(PMI-NC)$ [0.64]	
	264 (0.12)	
	$\pi(PMI)_H \rightarrow \pi^*(PMI)$ [0.48]	
CHCl ₃	$\pi(PMI)_H \rightarrow \pi^*(PMI-NC)_L$ [0.30]	
	527 (1.08)	493 (0.79)
	$\pi(PMI)_H \rightarrow \pi^*(PMI-NC)_L$ [0.71]	$\pi(Per)_H \rightarrow \pi^*(Per-NC)_L$ [0.70]
	332 (0.08)	297 (0.14)
	$\pi(PMI) \rightarrow \pi^*(PMI-NC)_L$ [0.46]	$\pi(C_6F_5) \rightarrow \pi^*(Per-NC)$ [0.49]
	$\pi(PMI) \rightarrow \pi^*(PMI-NC)_L$ [0.37]	266 (0.30)
	292 (0.16)	$\pi(Per) \rightarrow \pi^*(Per-NC)_L$ [0.44]
	$\pi(PMI)_H \rightarrow \pi^*(PMI)$ [0.40]	$\pi(Per)_H \rightarrow \pi^*(Per-NC)$ [0.39]
	$\pi(C_6F_5) \rightarrow \pi^*(PMI-NC)_L$ [0.37]	262 (0.23)
	288 (0.10)	$\pi(Per) \rightarrow \pi^*(Per-NC)_L$ [0.52]
$\pi(C_6F_5) \rightarrow \pi^*(PMI-NC)_L$ [0.59]	$\pi(PMI)_H \rightarrow \pi^*(PMI)$ [0.27]	$\pi(Per)_H \rightarrow \pi^*(Per-NC)$ [0.33]
	264 (0.15)	
	$\pi(PMI)_H \rightarrow \pi^*(PMI-NC)$ [0.53]	
	$\pi(PMI) \rightarrow \pi^*(PMI-NC)_L$ [0.34]	

Table S2. Calculated absorption peaks for $[M(CO)_5(CNR)]$ ($M = Cr, Mo, W; R = PMI, Per$).

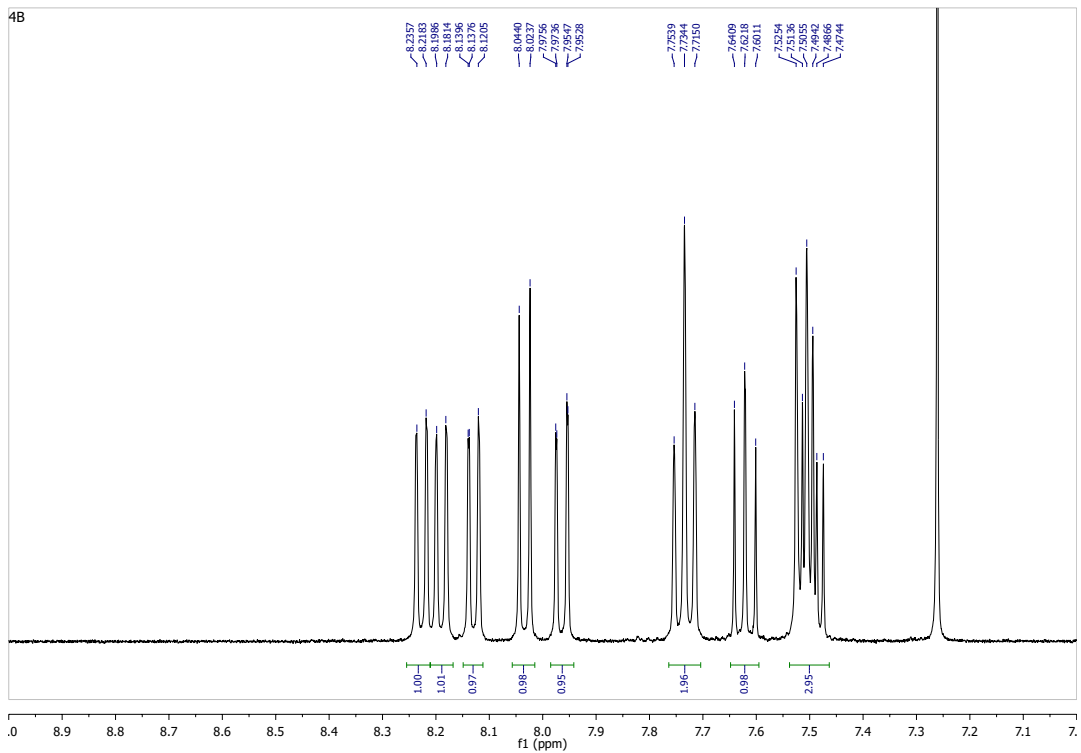
R-X	Cr(CO) ₅		Mo(CO) ₅		W(CO) ₅	
	Gas phase	CHCl ₃	Gas phase	CHCl ₃	Gas phase	CHCl ₃
PMI-NC-X $\lambda(f)$	518 (0.97)	536 (1.14)	526 (0.99)	542 (1.19)	530 (1.02)	547 (1.22)
	281 (0.08)	282 (0.10)	299 (0.16)	300 (0.16)	303 (0.12)	305 (0.14)
	266 (0.09)	264 (0.12)	266 (0.07)	282 (0.07)	269 (0.12)	268 (0.20)
			264 (0.06)	267 (0.11)	265 (0.07)	266 (0.10)
				266 (0.13)		
Per-NC-X $\lambda(f)$	468 (0.70)	482 (0.84)	474 (0.75)	487 (0.90)	477 (0.78)	492 (0.93)
	259 (0.15)	265 (0.19)	285 (0.11)	286 (0.10)	286 (0.10)	287 (0.09)
		262 (0.22)	261 (0.24)	264 (0.37)	262 (0.22)	265 (0.34)
			256 (0.08)	259 (0.05)	259 (0.07)	

Fig. S5 ^1H and ^{19}F NMR spectra

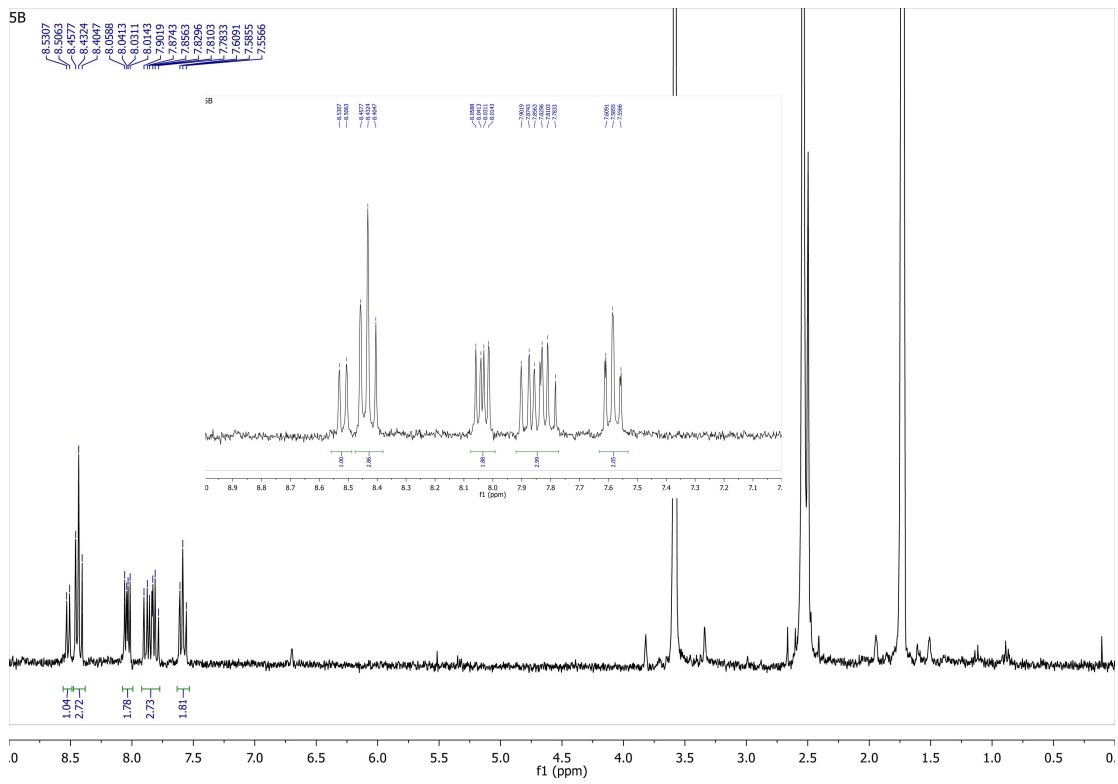
4a

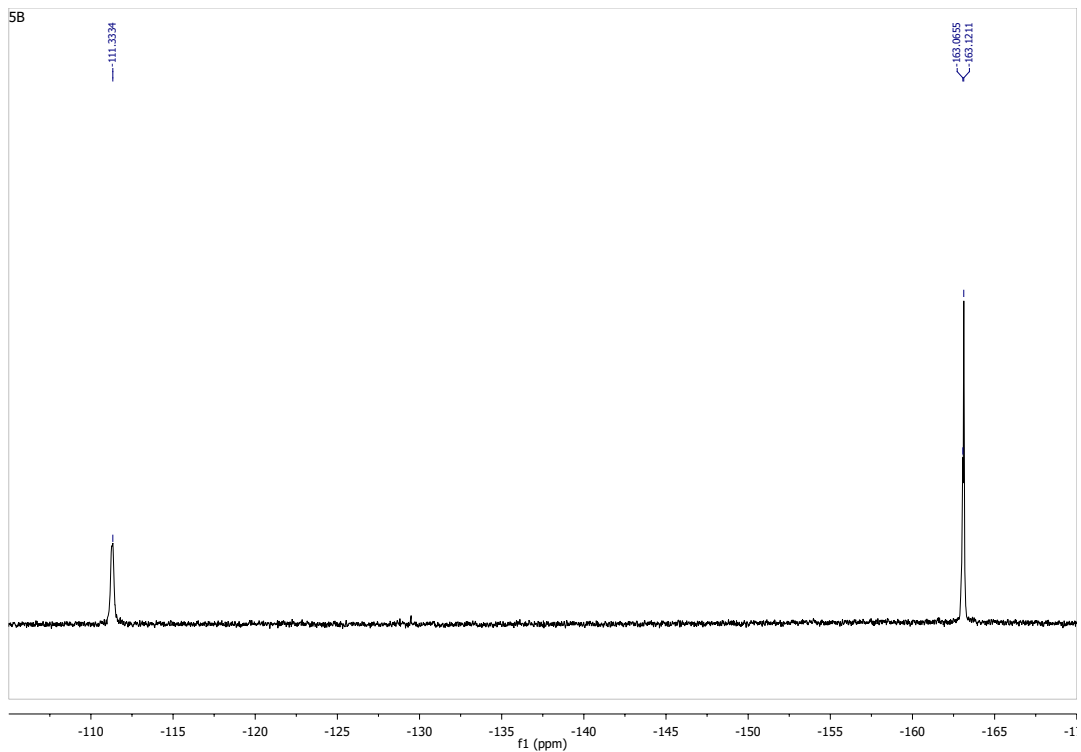


4b

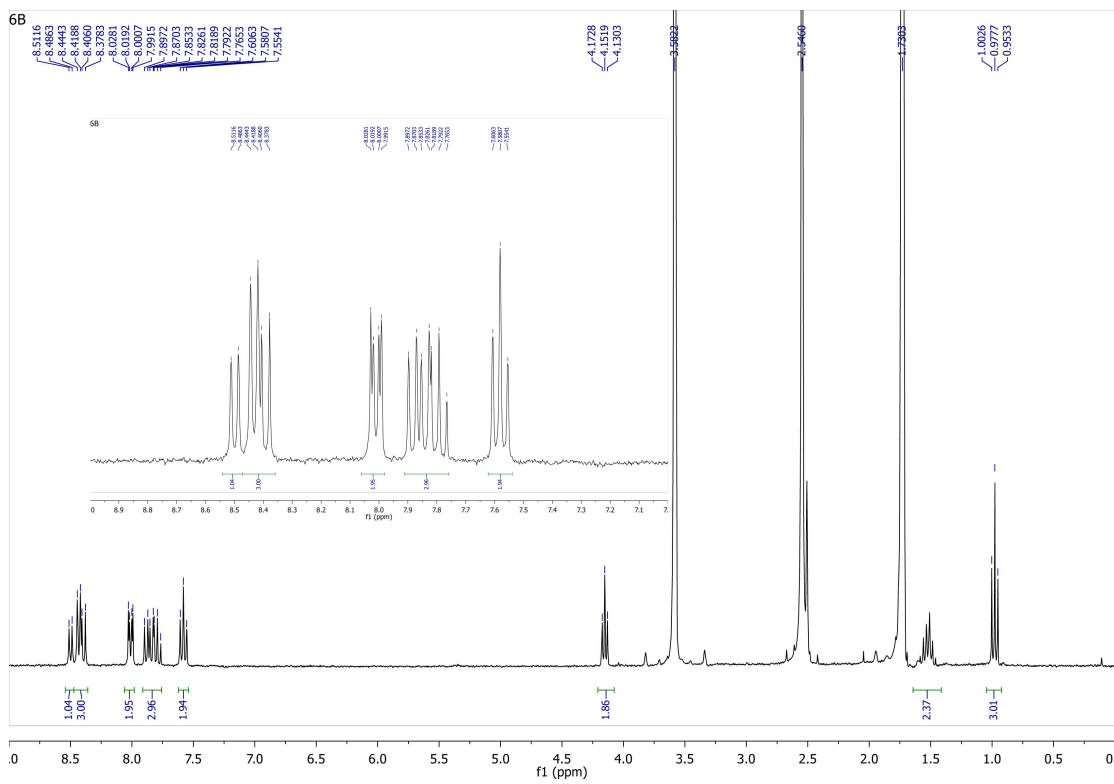


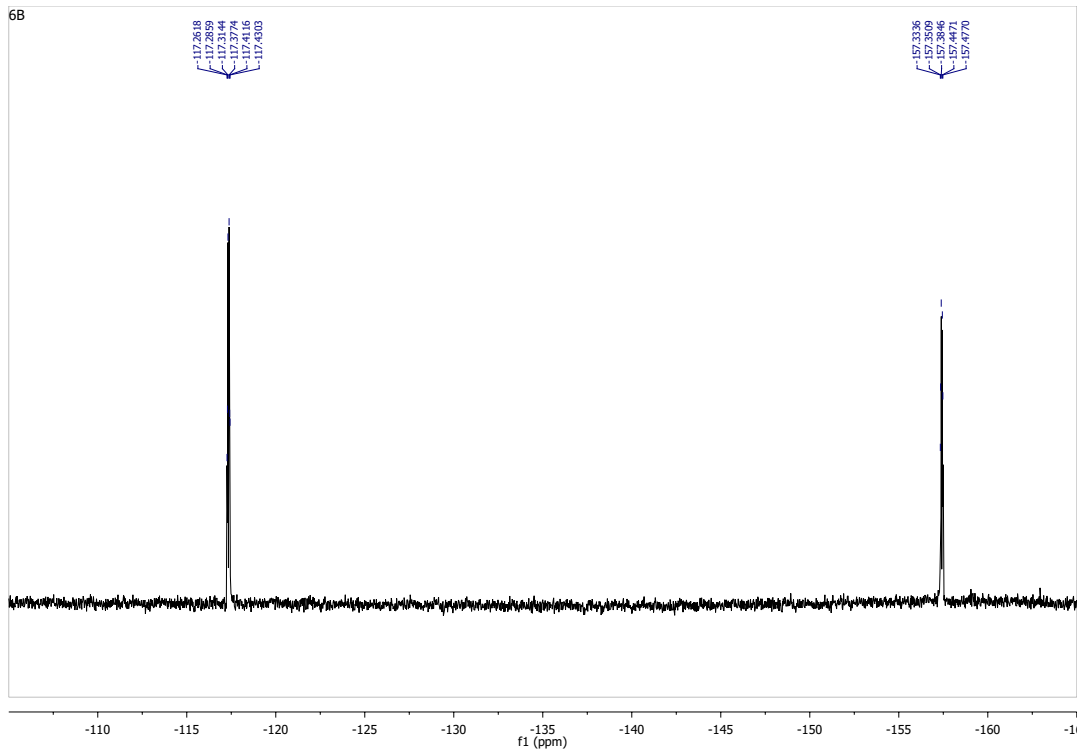
5b



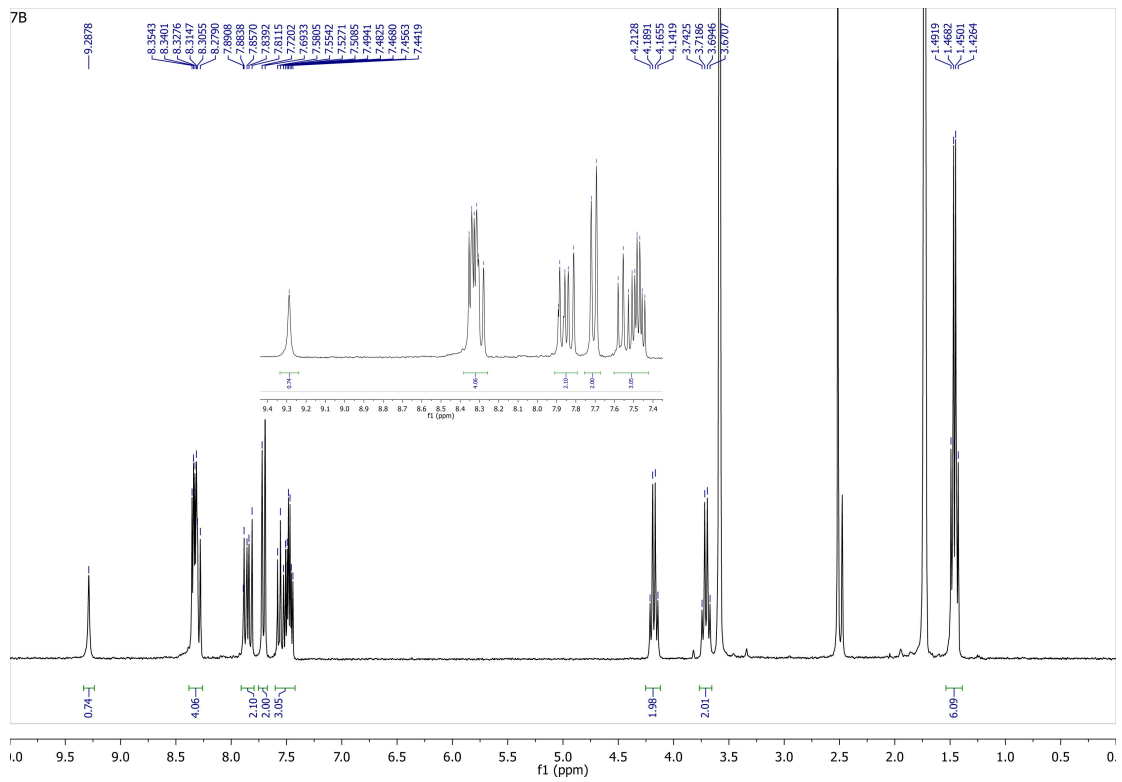


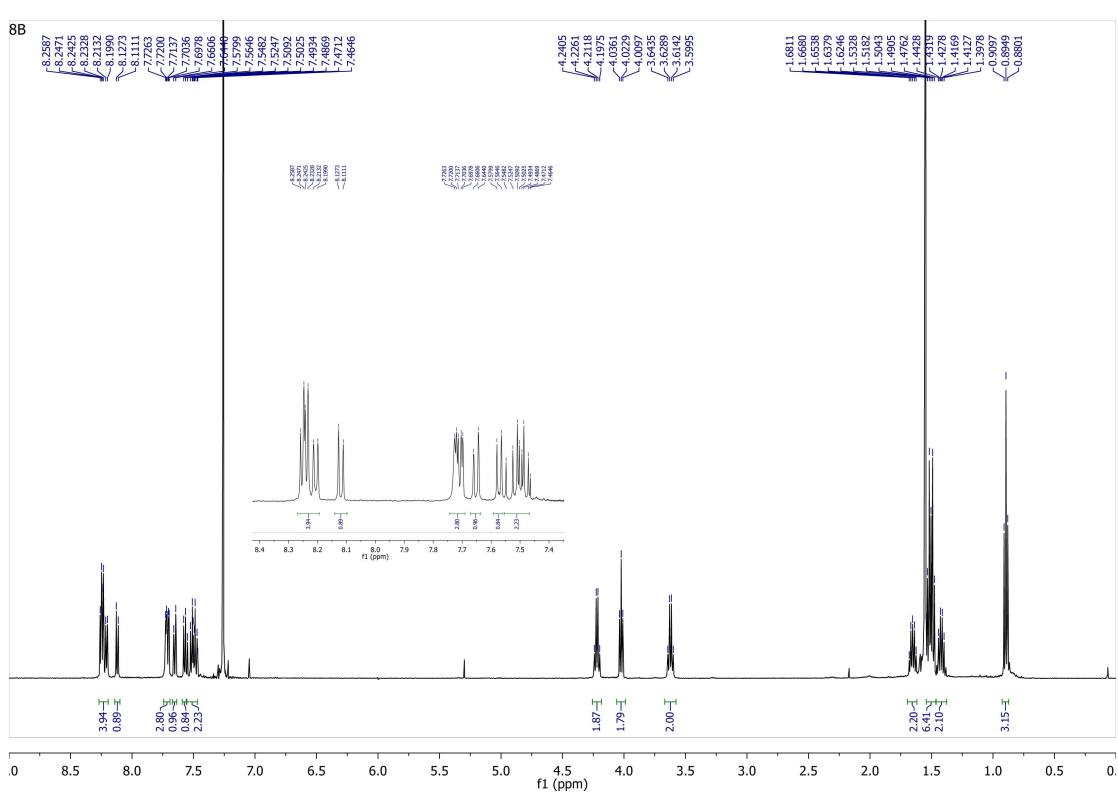
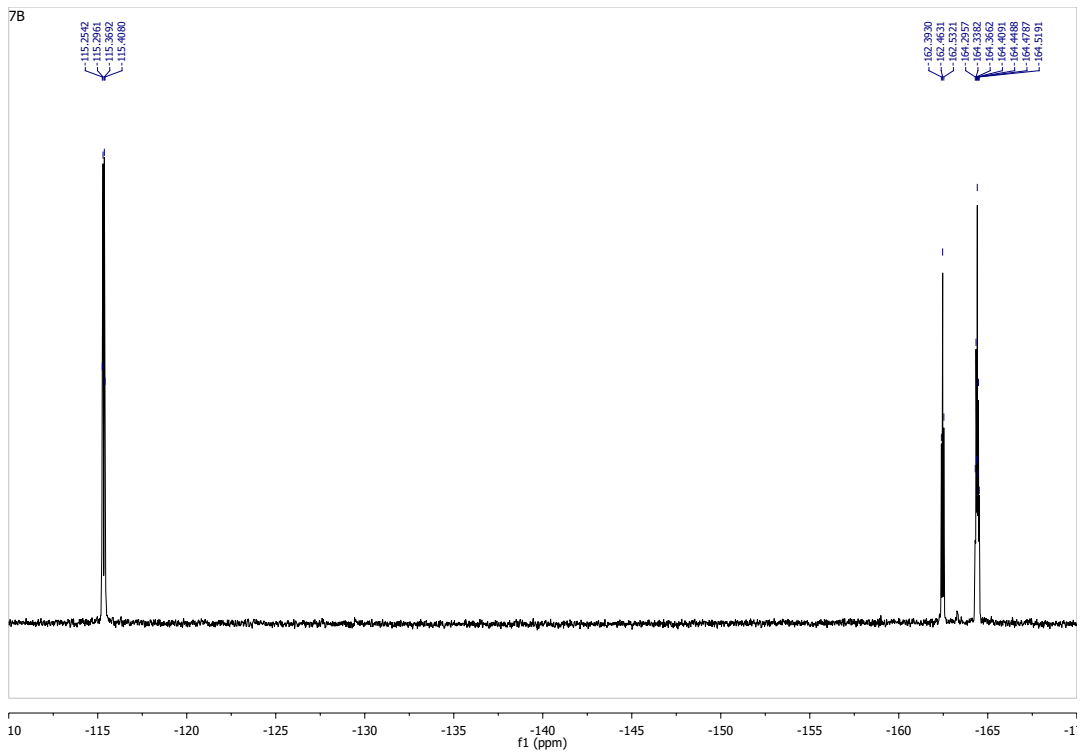
6b

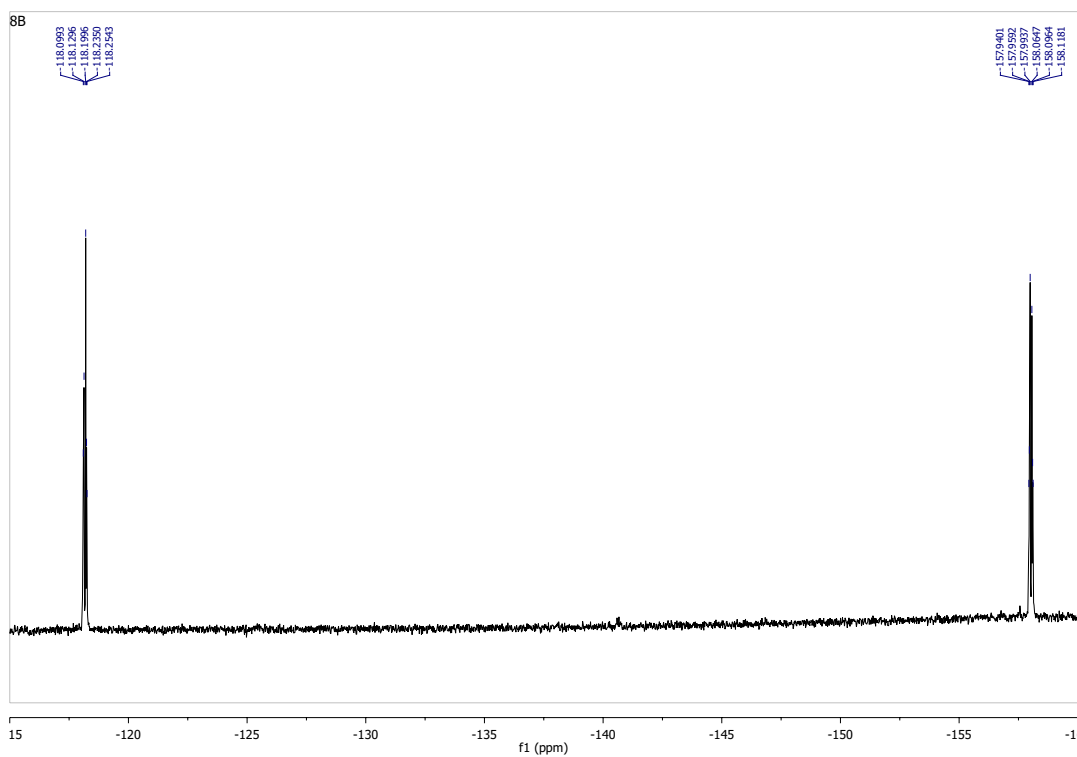
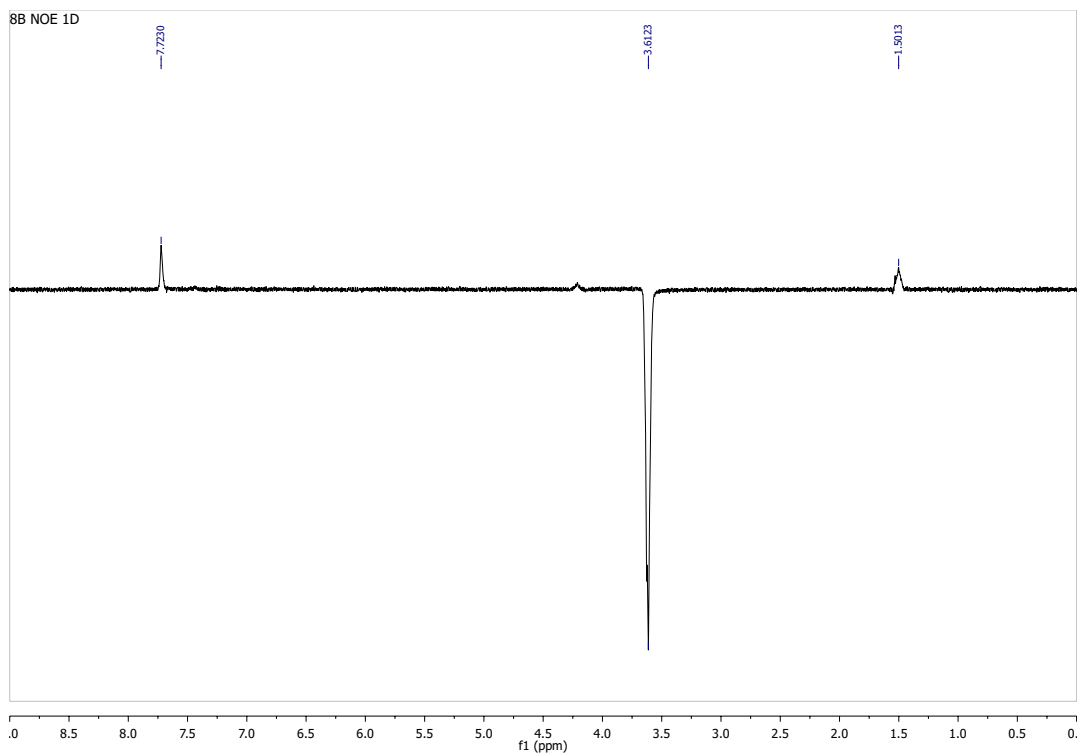




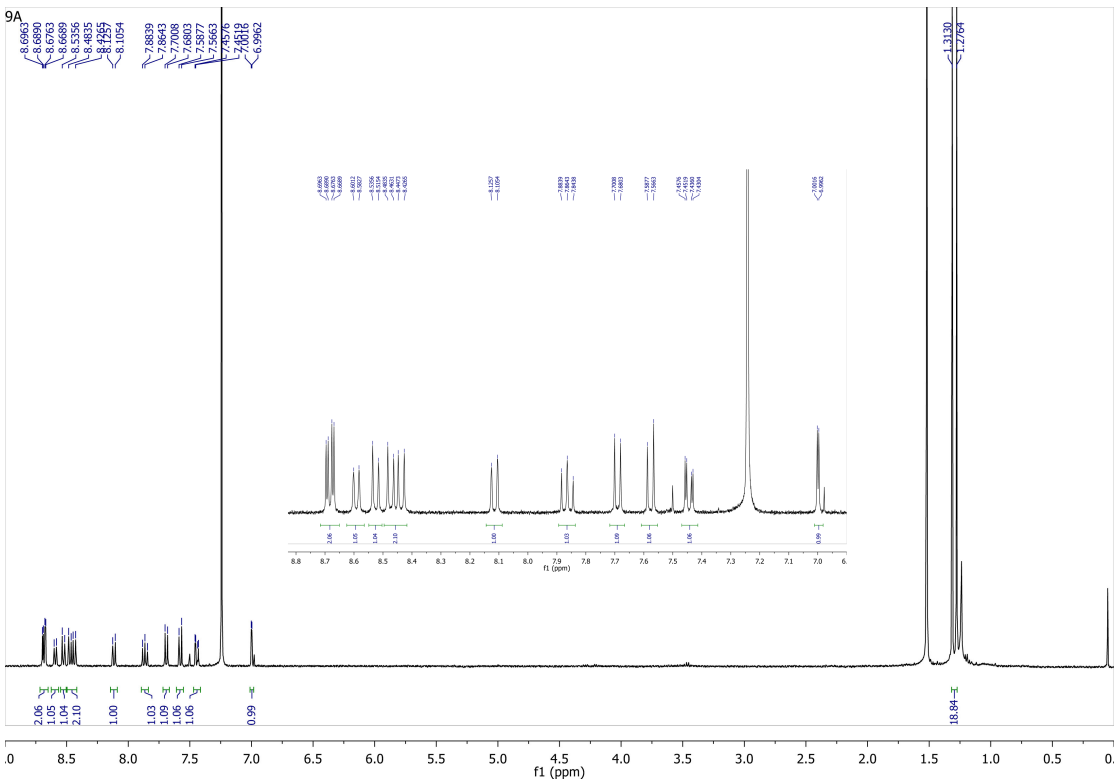
7b



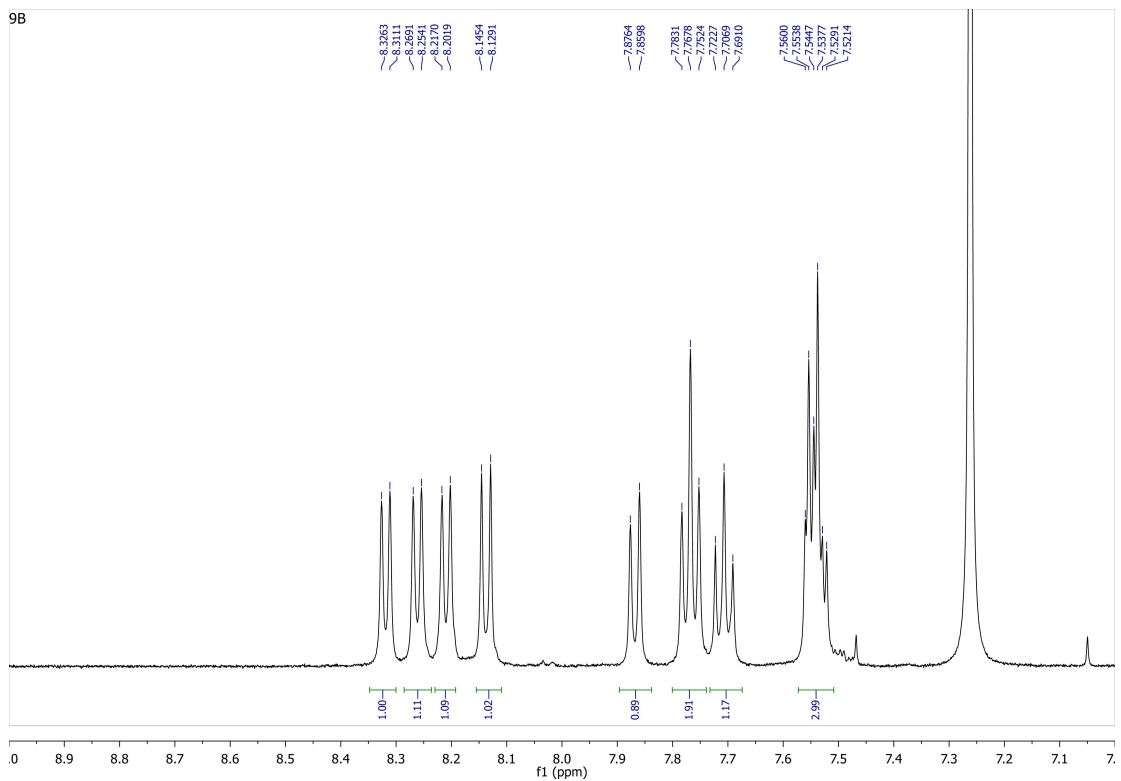




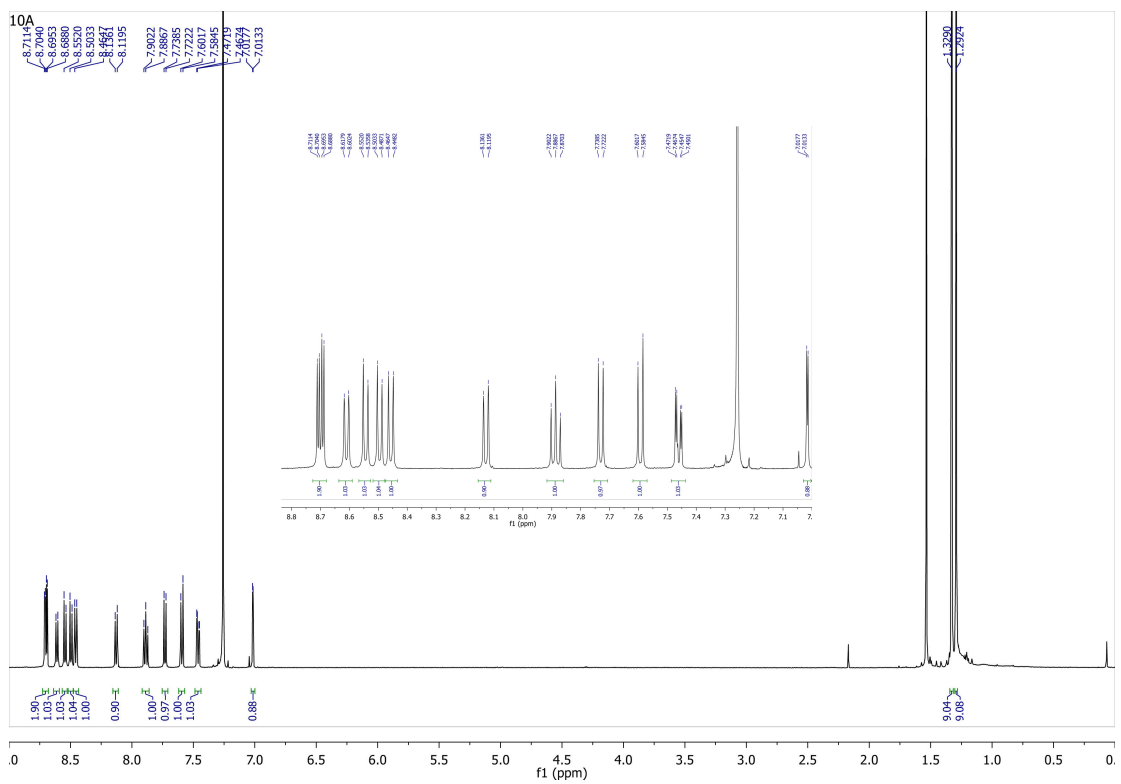
9a



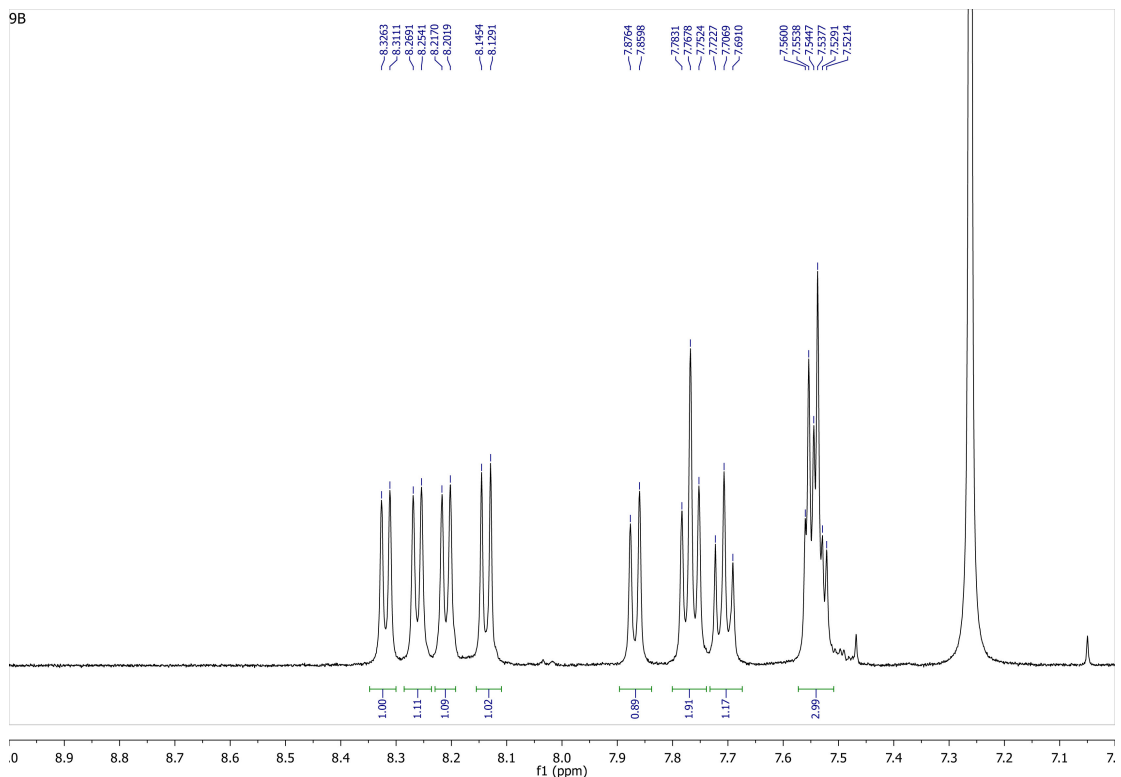
9b



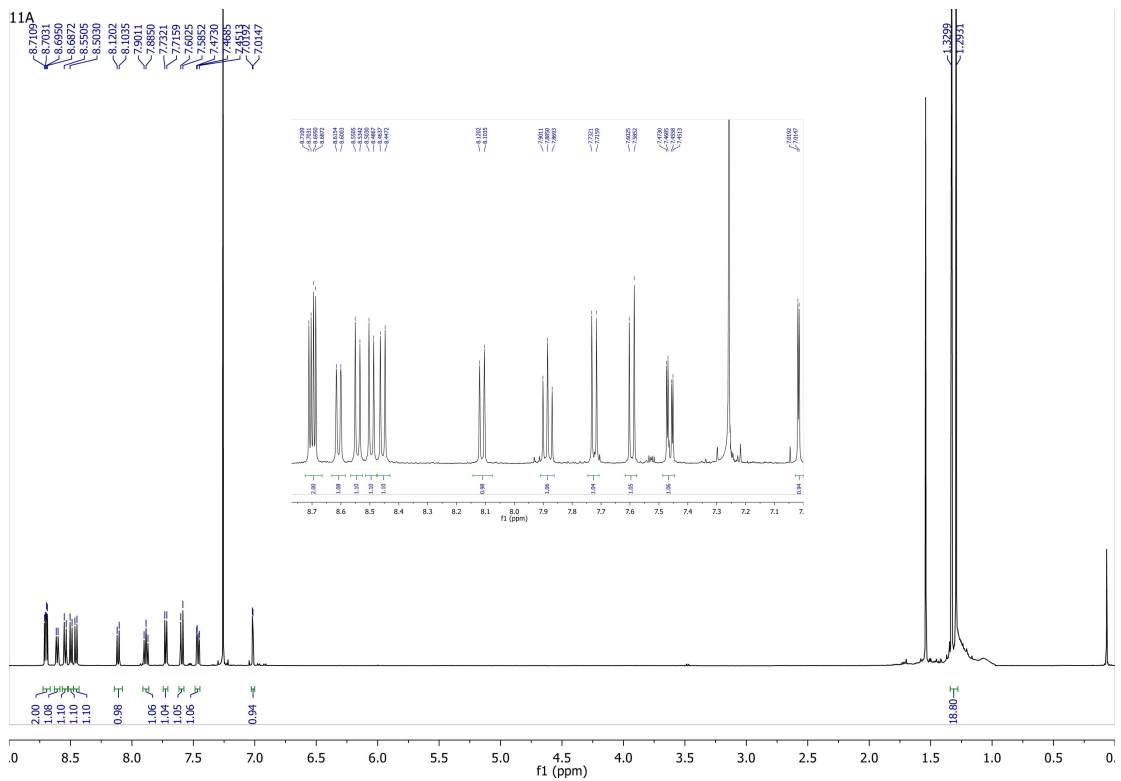
10a



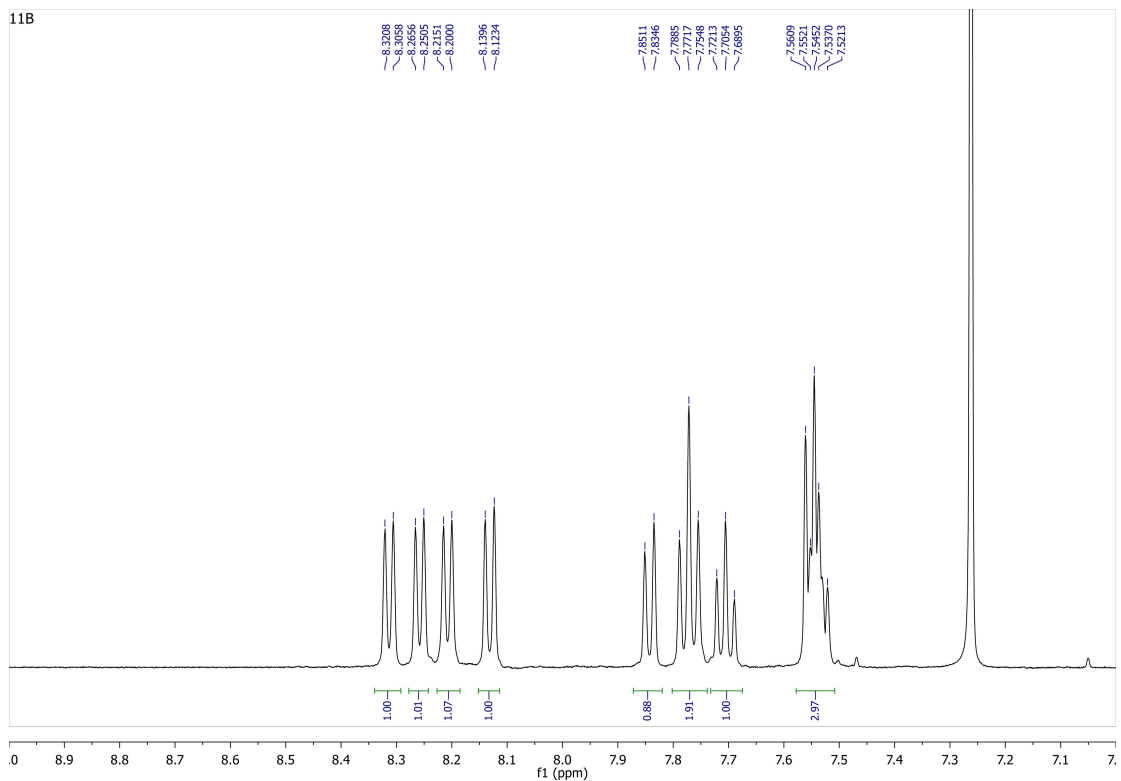
10b



11a



11b



12a

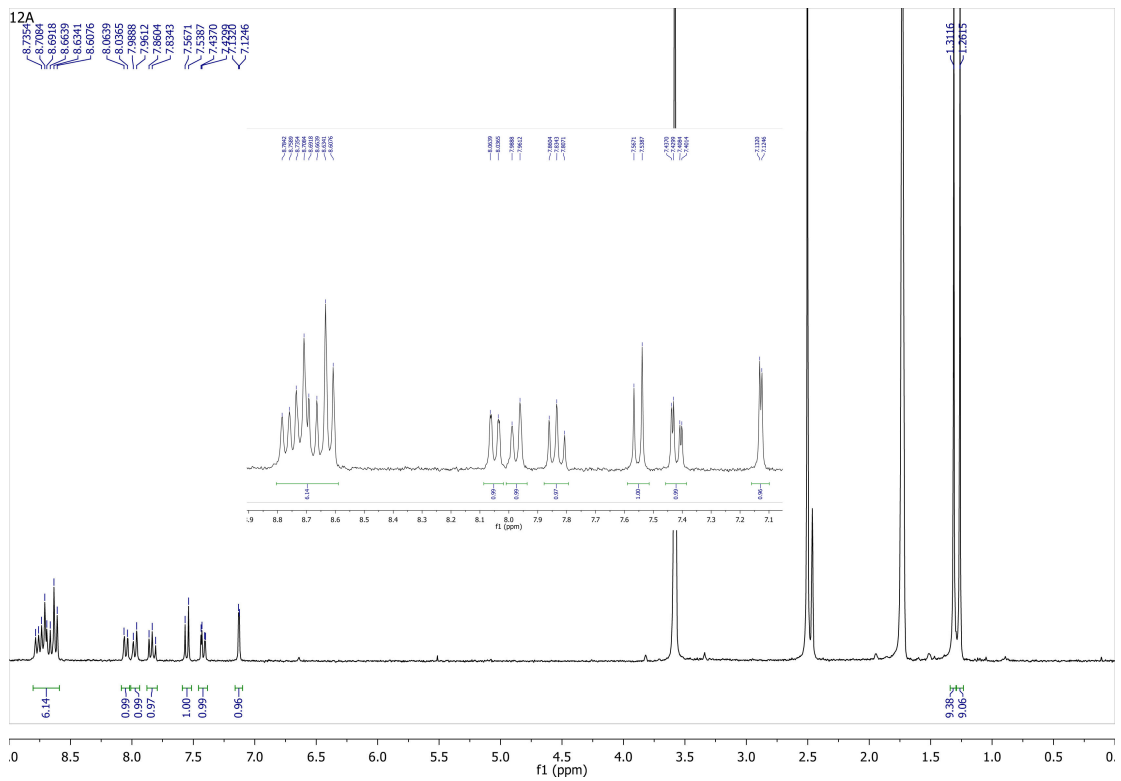
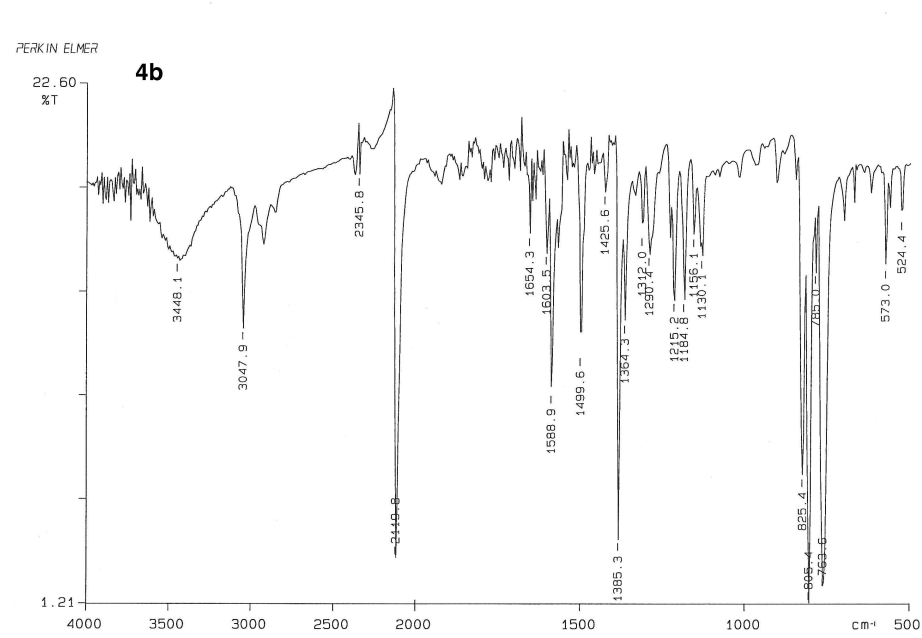
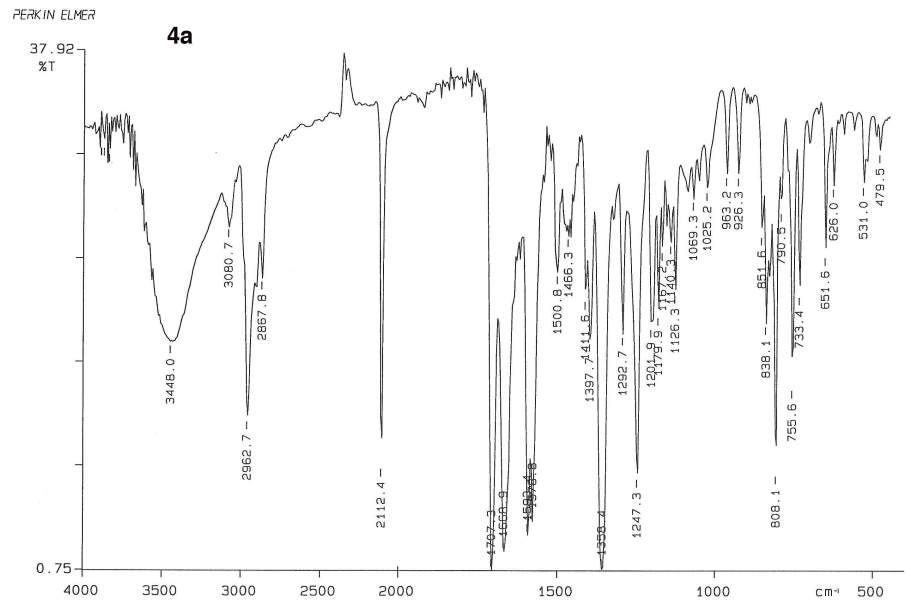
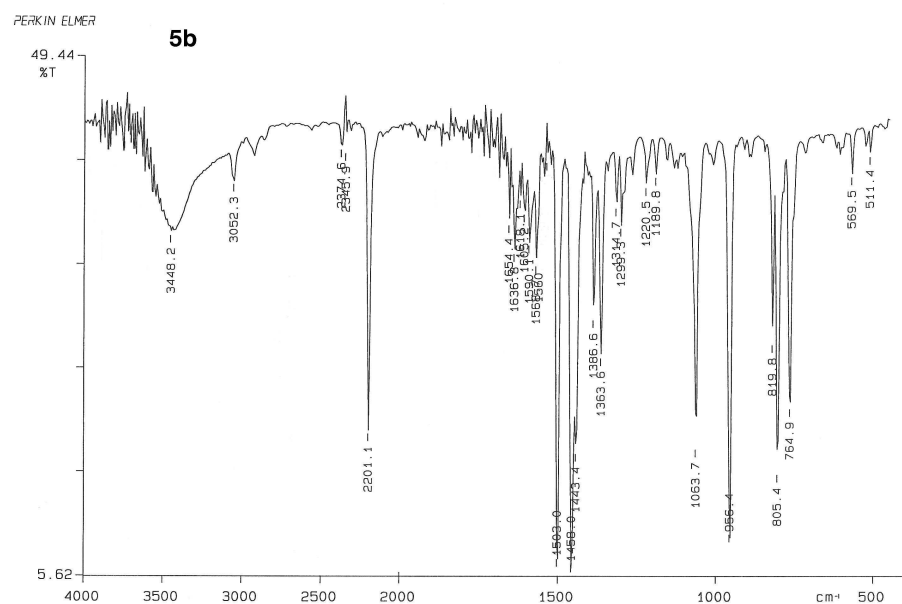
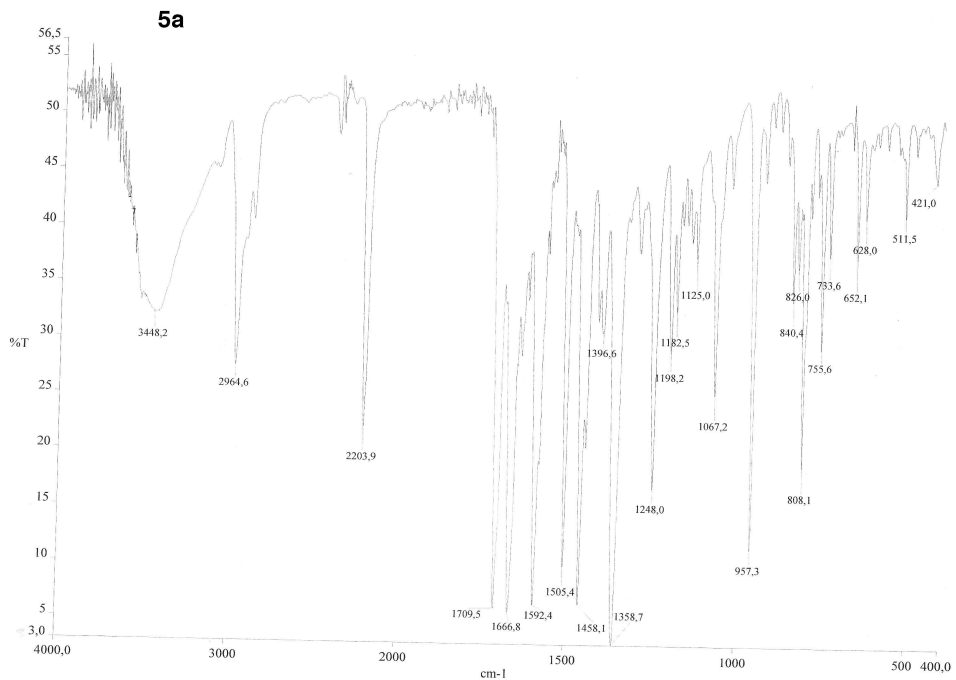
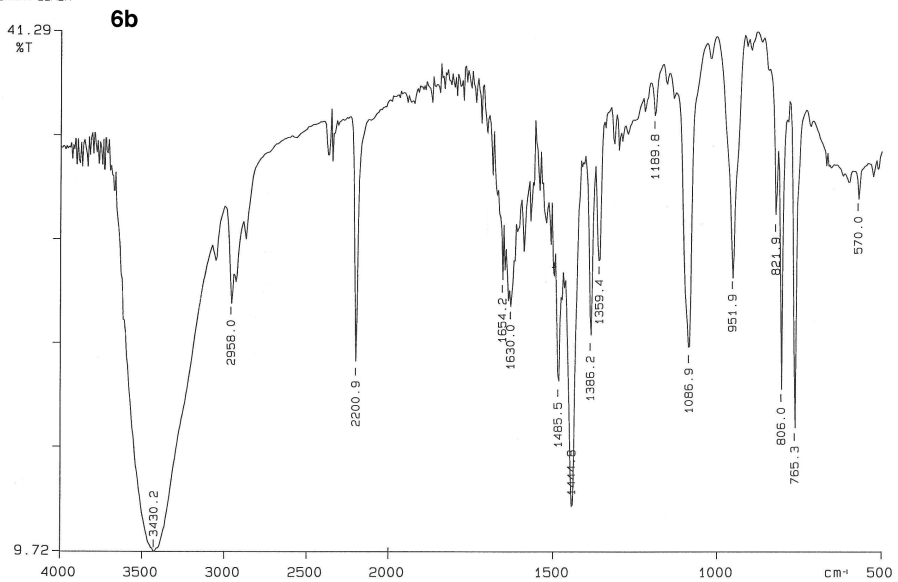
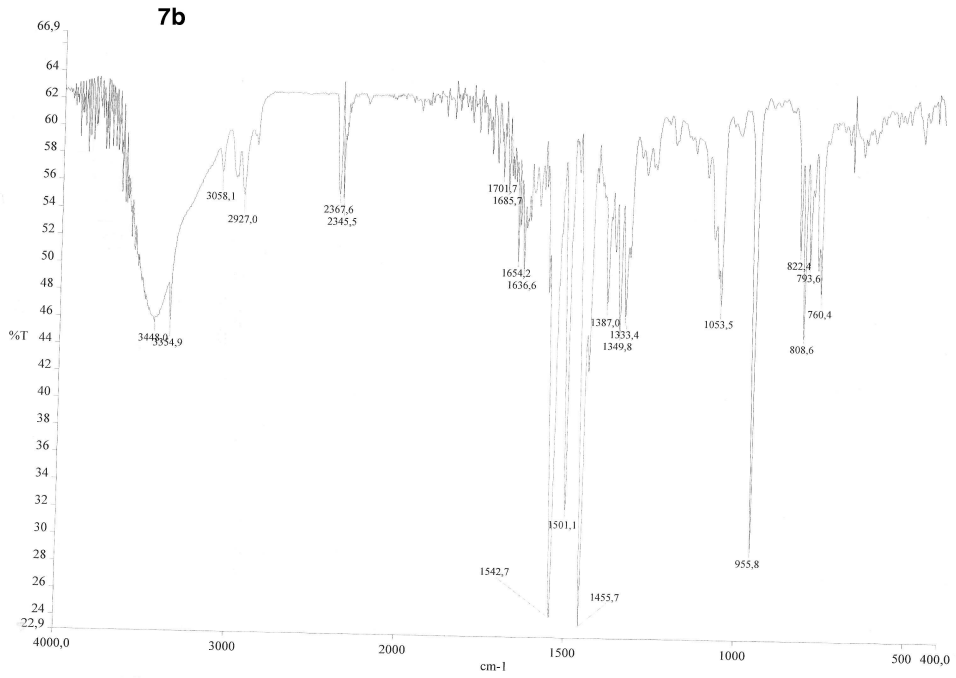


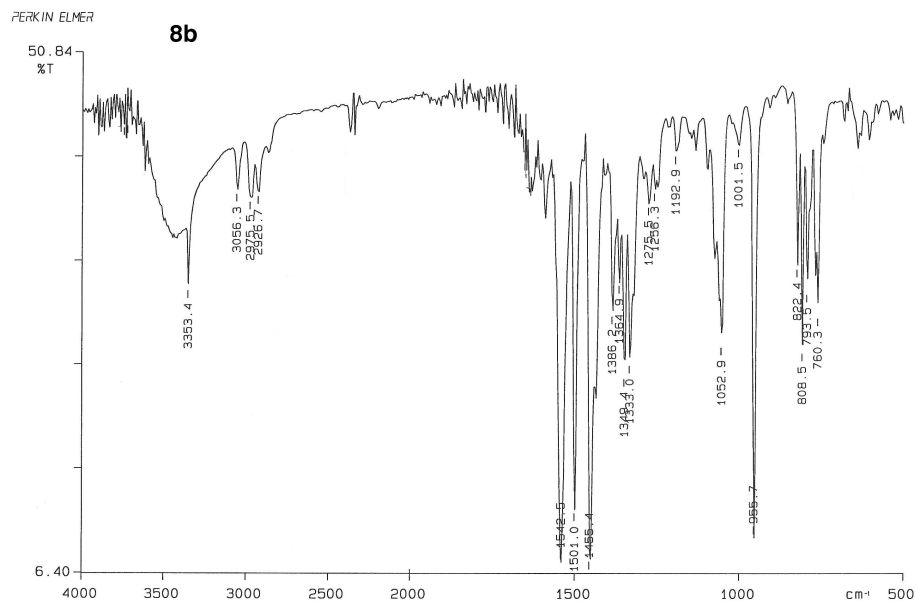
Fig. S6. IR spectra



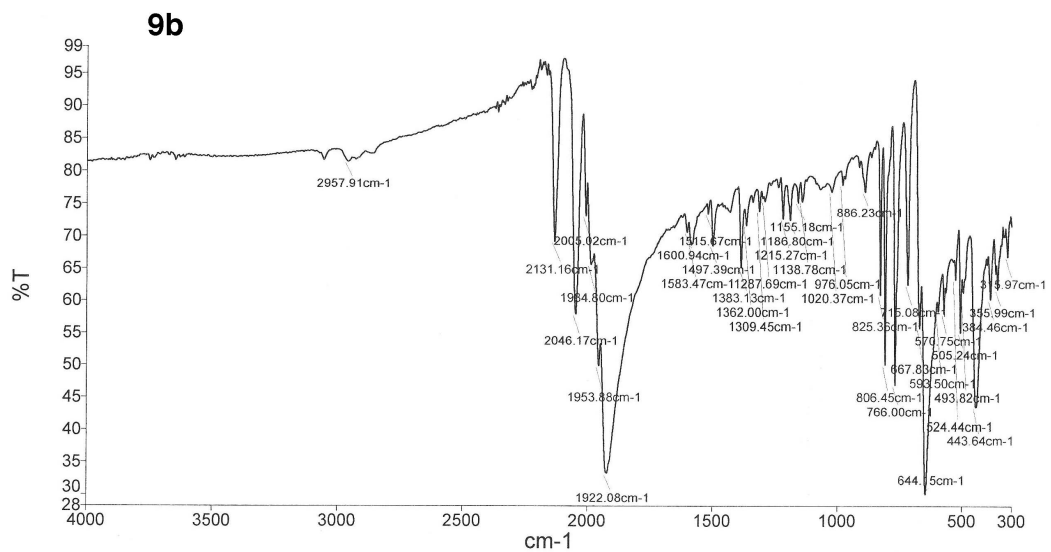


PERKIN ELMER

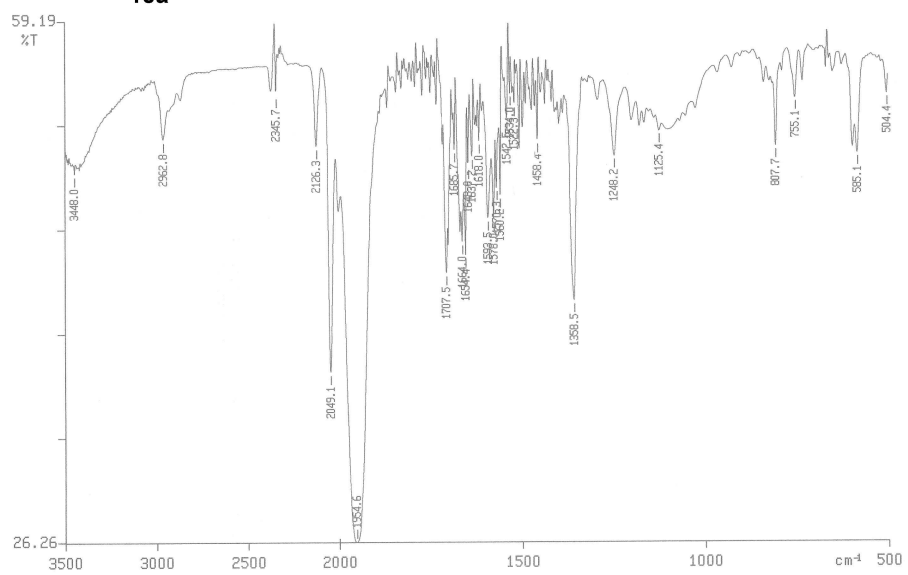
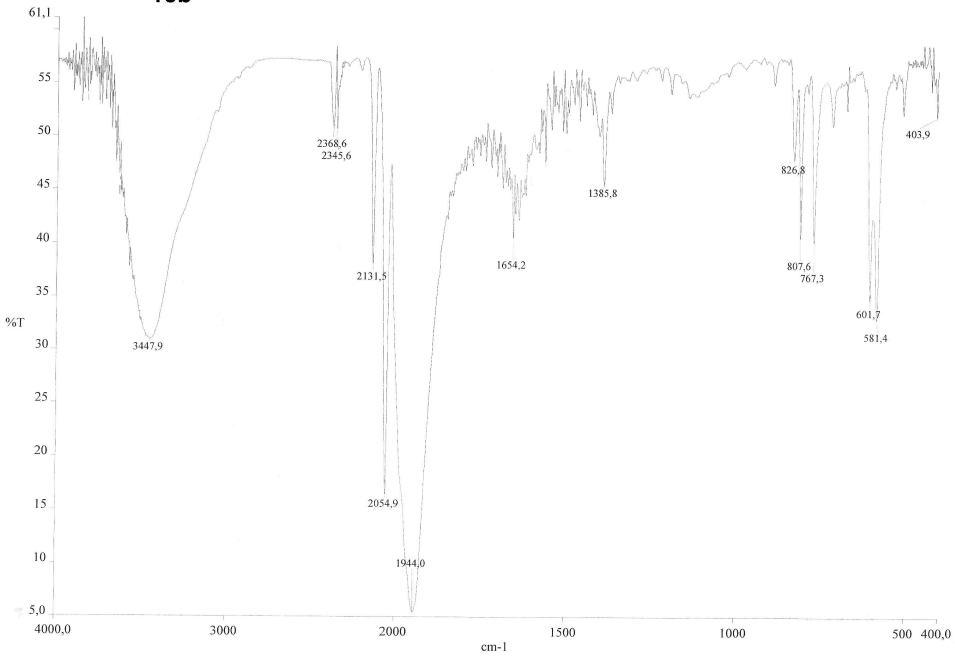
6b**7b**



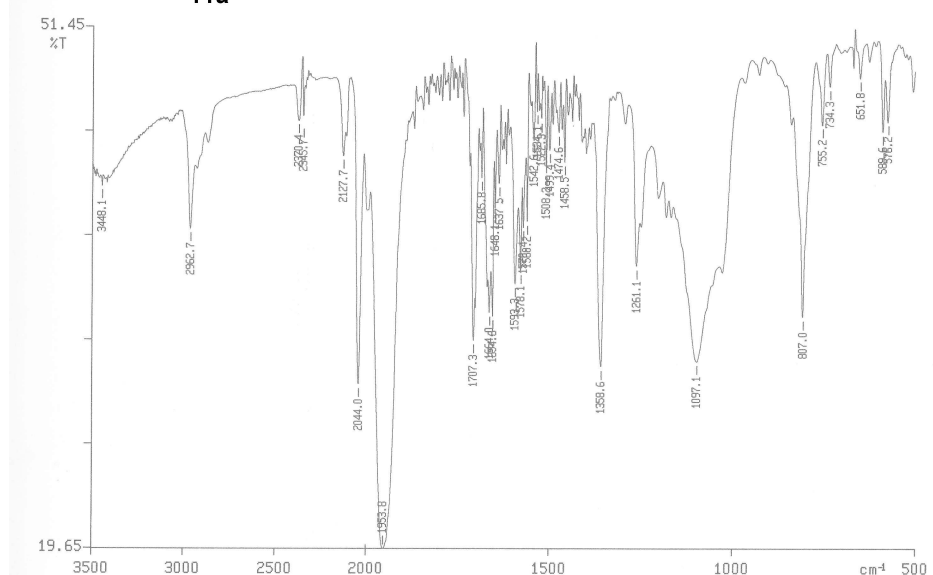
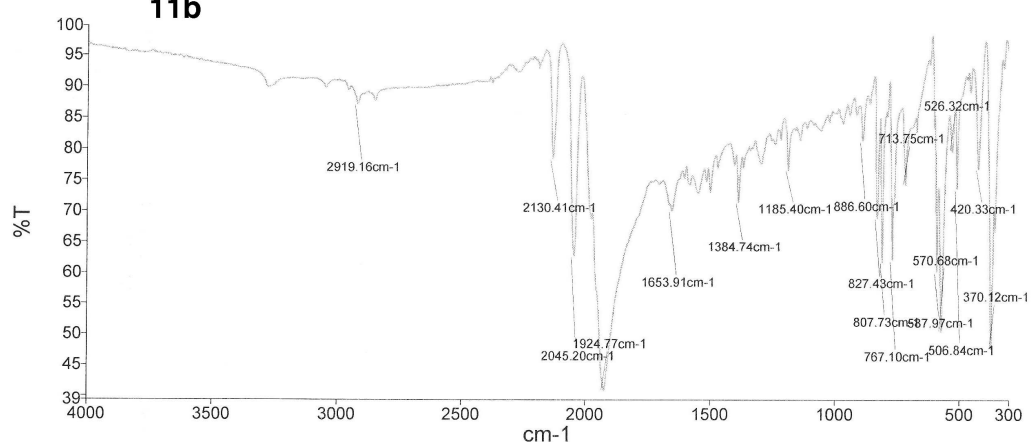
08/04/22 13:44
X: 4 scans, 4.0 cm^{-1} , flat

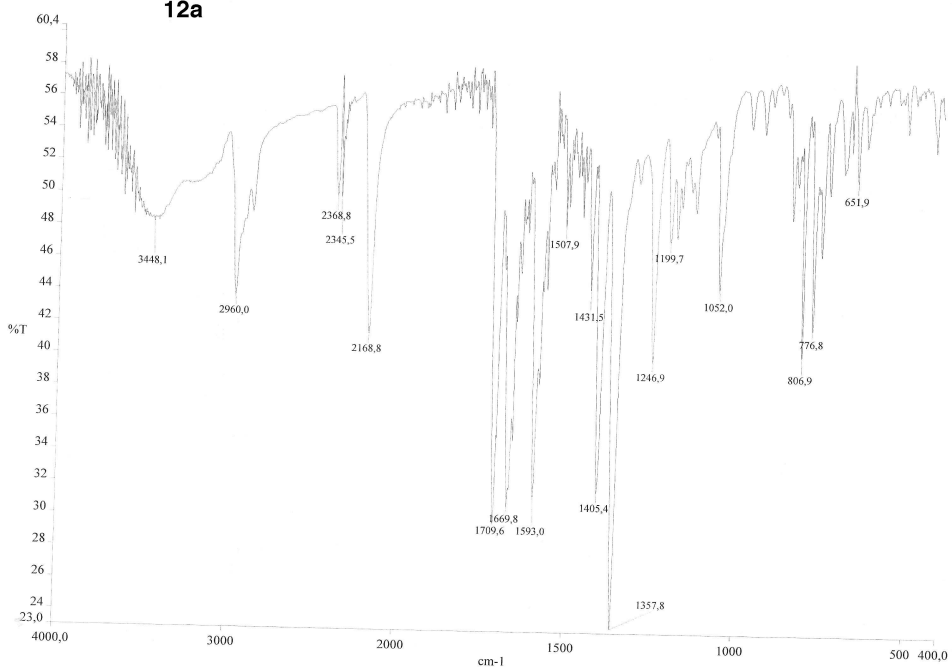


PERKIN ELMER

10a**10b**

PERKIN ELMER

11a**11b**

12a

PERKIN ELMER

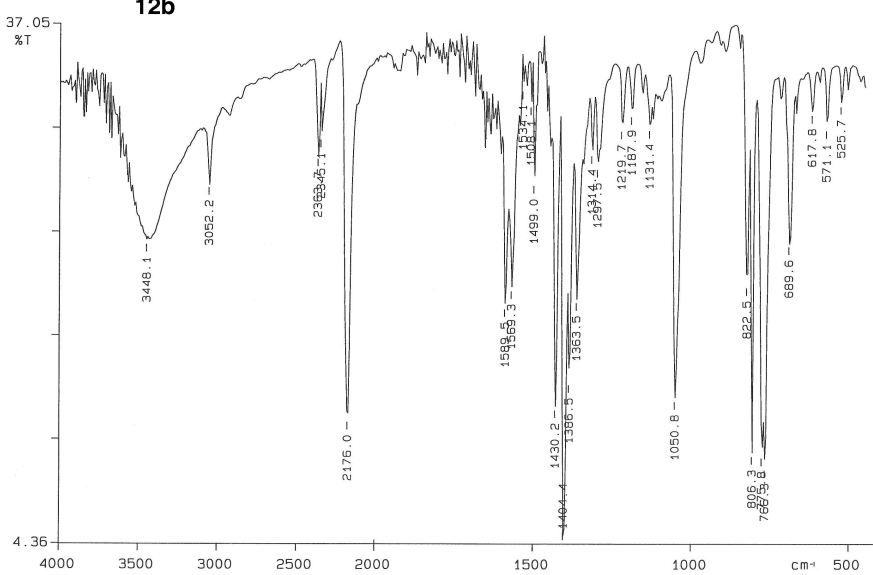
12b

Fig. S7. Fluorescence decays in dichloromethane, at room temperature

Mono-exponential and bi-exponential fluorescence decay models were fitted to each decay. Eqn (1) describes the mono-exponential decay model:

$$I(t) = I_0 \cdot \exp(-t/\tau) \quad (1)$$

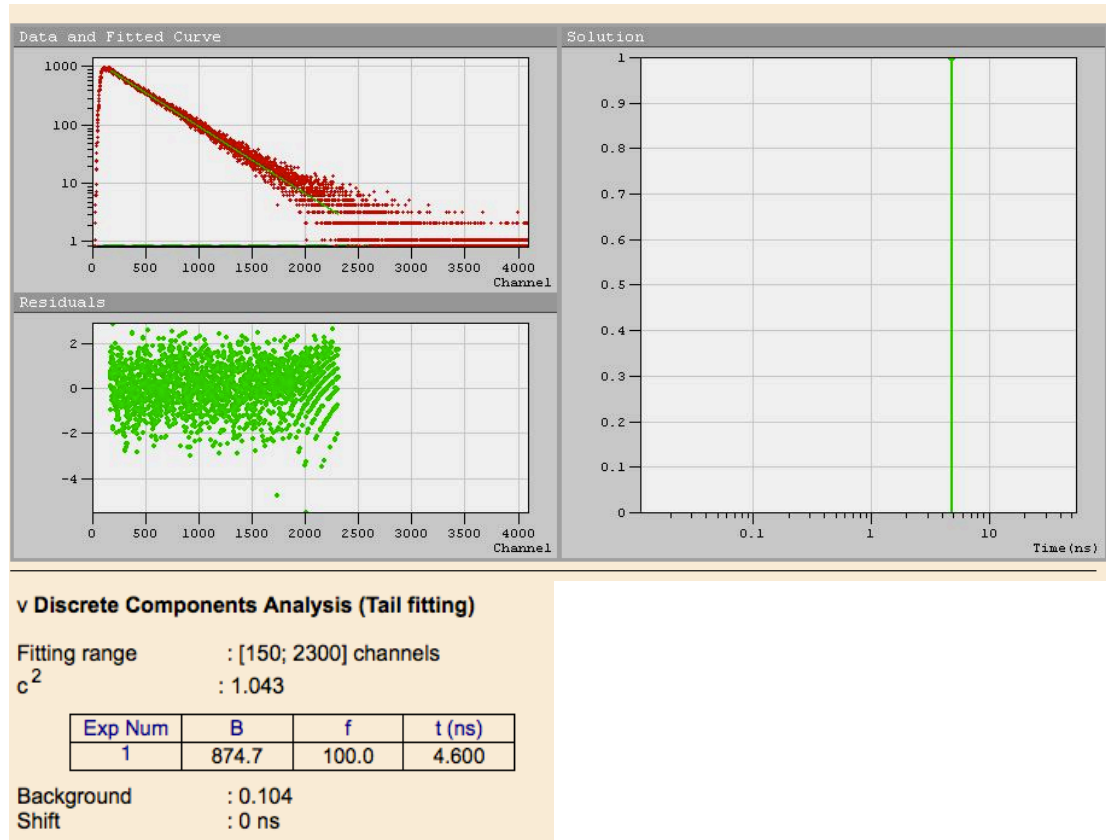
where I_0 is the relative intensity, t is the time and τ is the fluorescence lifetime, both expressed in ns. The bi-exponential decay model is expressed by Equation (2) as:

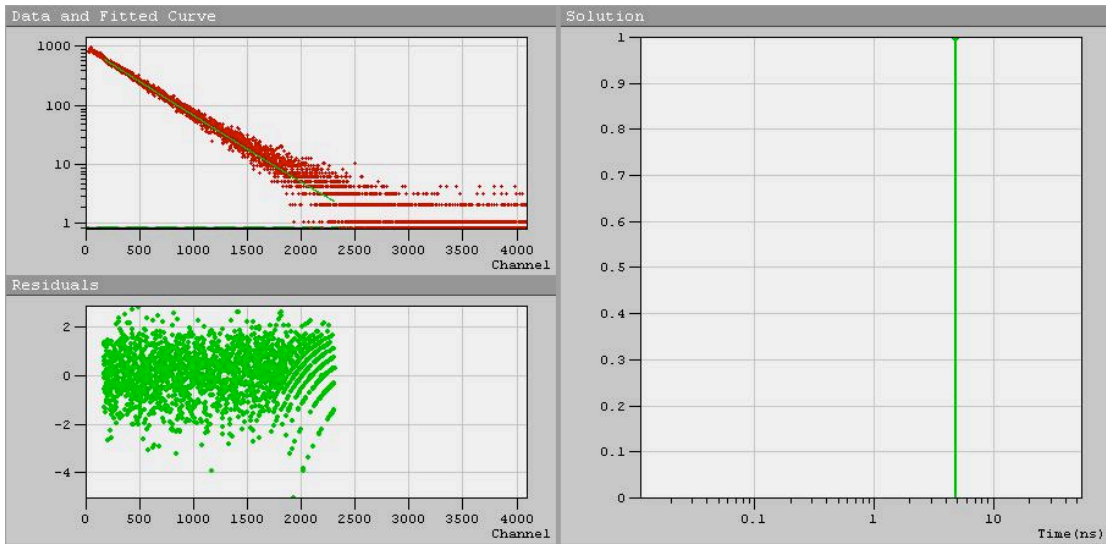
$$I(t) = A + B_1 \cdot \exp(-t/\tau_1) + B_2 \cdot \exp(-t/\tau_2) \quad (2)$$

where B_1 and B_2 are the relative intensities associated with two lifetimes, τ_1 and τ_2 , respectively.

Mono-exponential models are normally used to fit fluorescence decay. Bi-exponential fits may be more appropriate for samples containing non-linear decays. Fitting was done using FAST software from Edinburgh Instruments by a least-squares algorithm using a deconvolution approach. In this method, convolution of Equation (1) or (2) with the instrumental response function (IRF) is done prior to evaluating the goodness of fit with a weighted χ^2 parameter.

4a



4b**v Discrete Components Analysis (Tail fitting)**

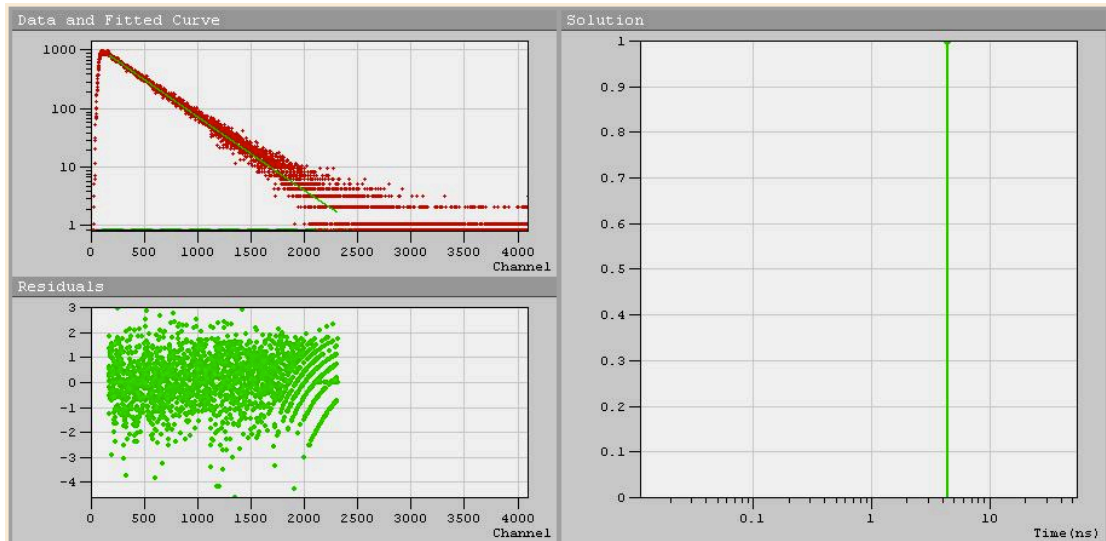
Fitting range : [150; 2300] channels

 c^2 : 1.013

Exp Num	B	f	t (ns)
1	618.6	100.0	4.626

Background : 0.288

Shift : 0 ns

5a**v Discrete Components Analysis (Tail fitting)**

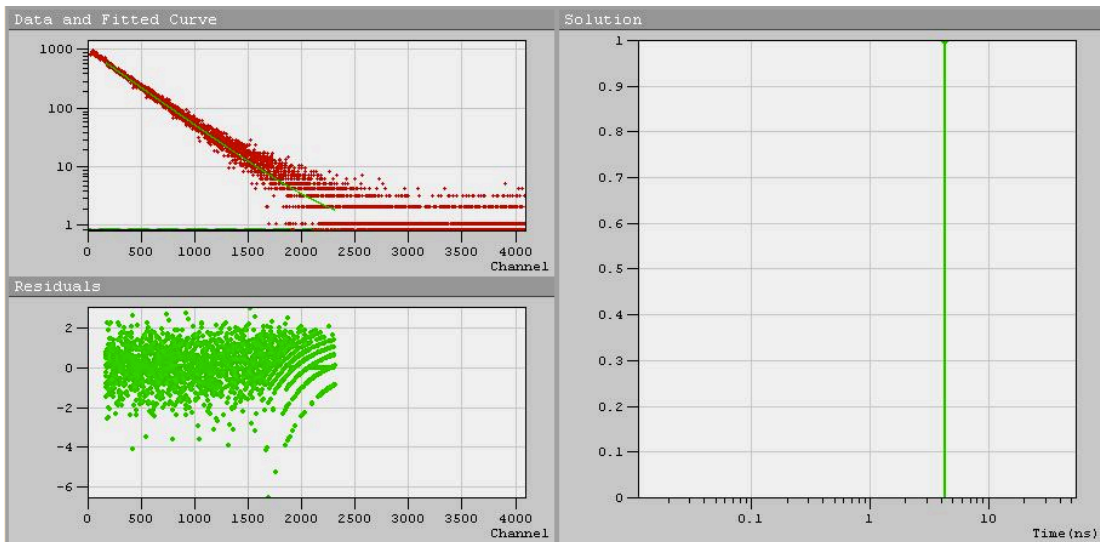
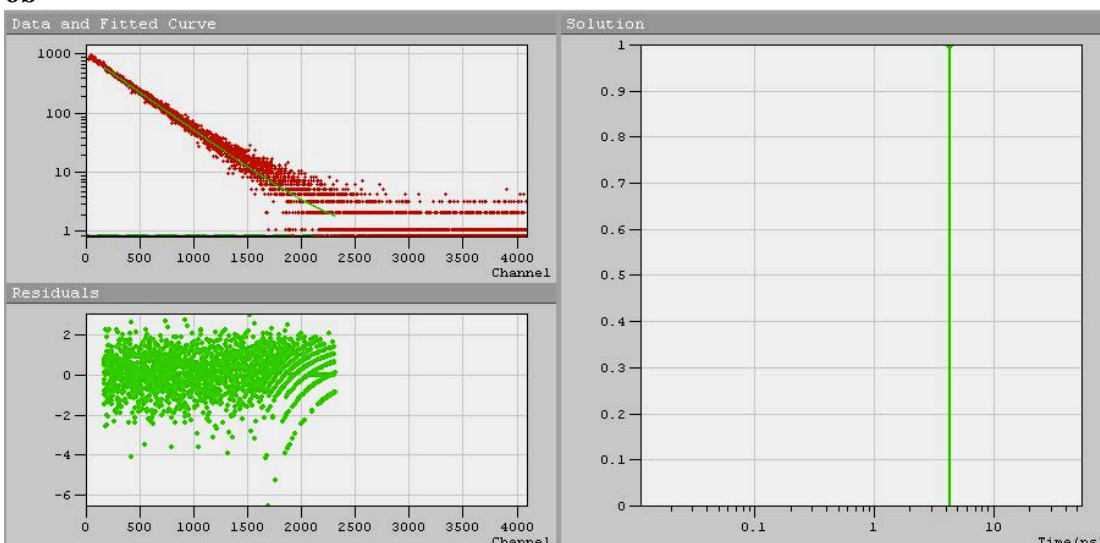
Fitting range : [150; 2300] channels

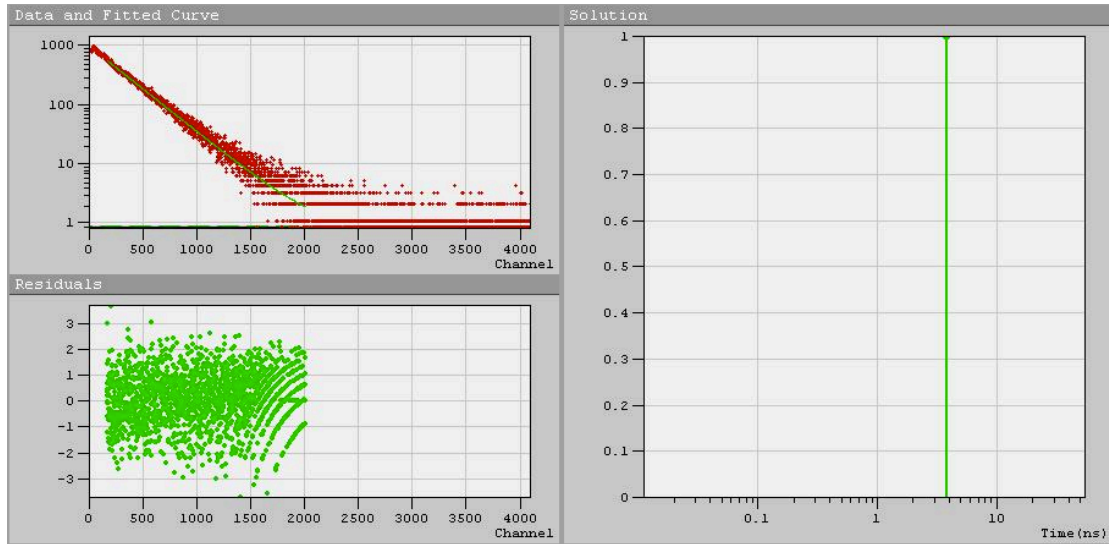
 c^2 : 1.027

Exp Num	B	f	t (ns)
1	834.6	100.0	4.188

Background : 0.138

Shift : 0 ns

5b**6b**

7b**v Discrete Components Analysis (Tail fitting)**

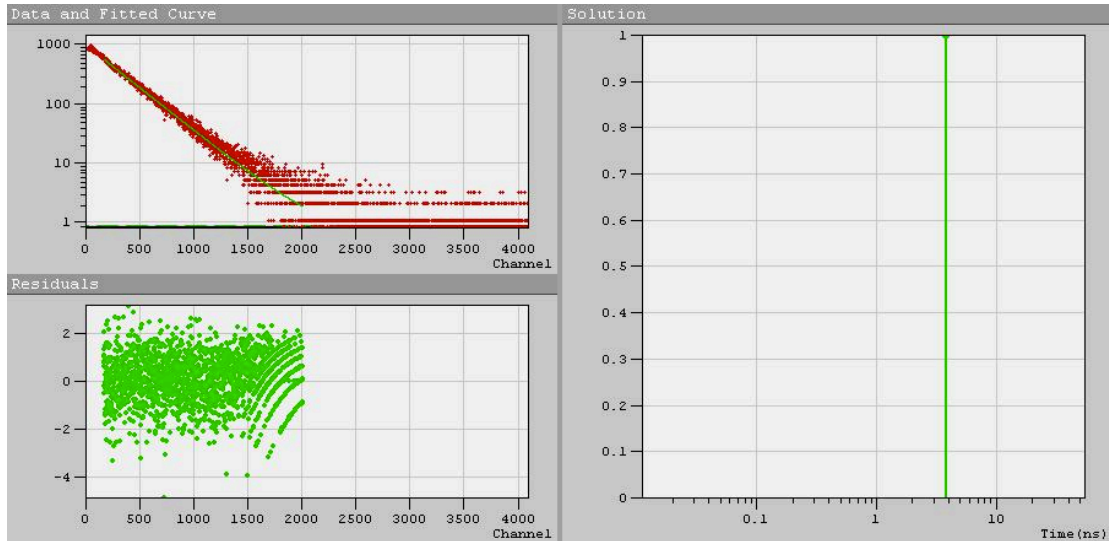
Fitting range : [150; 2000] channels

 c^2 : 1.032

Exp Num	B	f	t (ns)
1	562.8	100.0	3.670

Background : 0.669

Shift : 0 ns

8b**v Discrete Components Analysis (Tail fitting)**

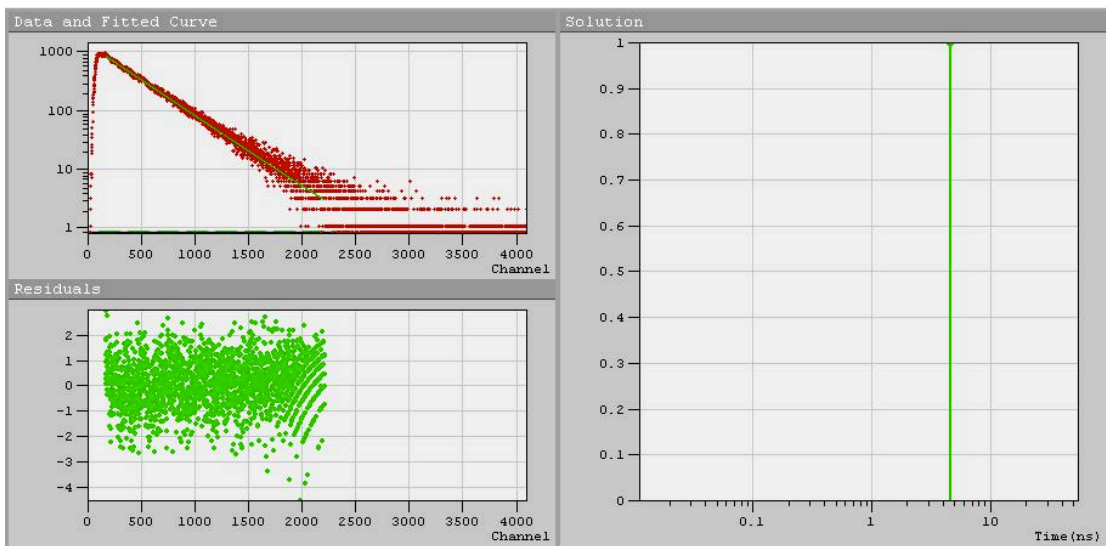
Fitting range : [150; 2000] channels

 c^2 : 1.032

Exp Num	B	f	t (ns)
1	562.8	100.0	3.670

Background : 0.669

Shift : 0 ns

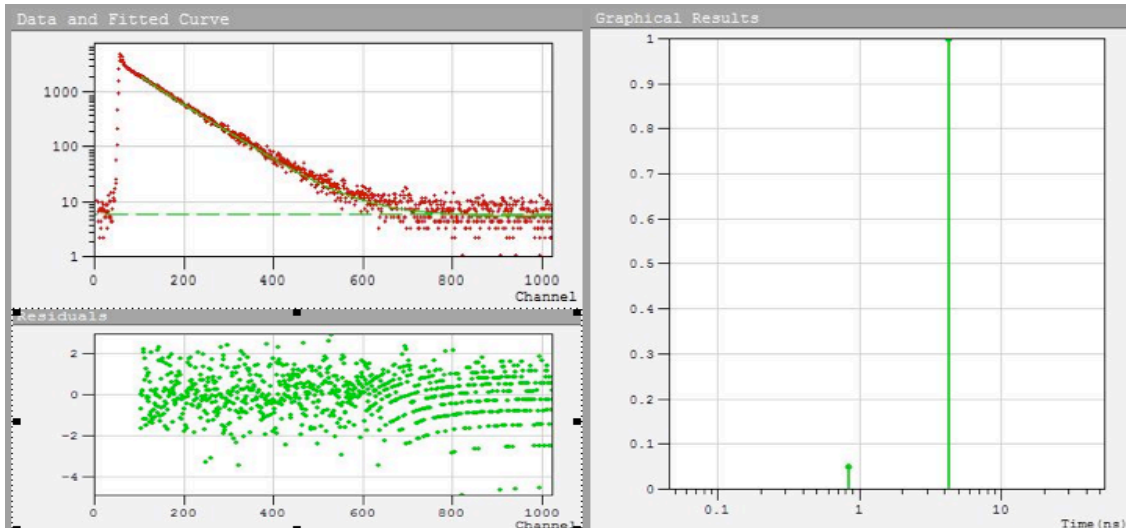
9a

❖ Discrete Components Analysis (Tail fitting)

Fitting range : [150; 2200] channels
 χ^2 : 1.013

Exp Num	B	f	t (ns)
1	848.4	100.0	4.388

Background : 0.206
Shift : 0 ns

9b

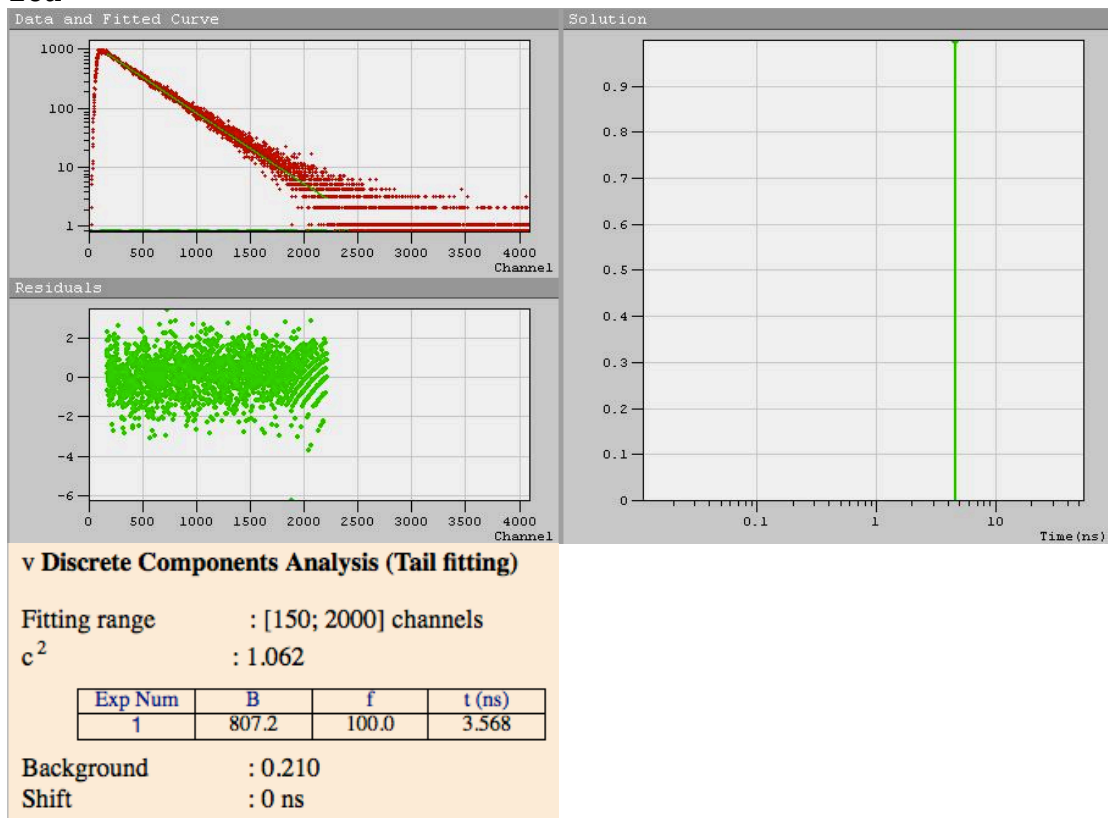
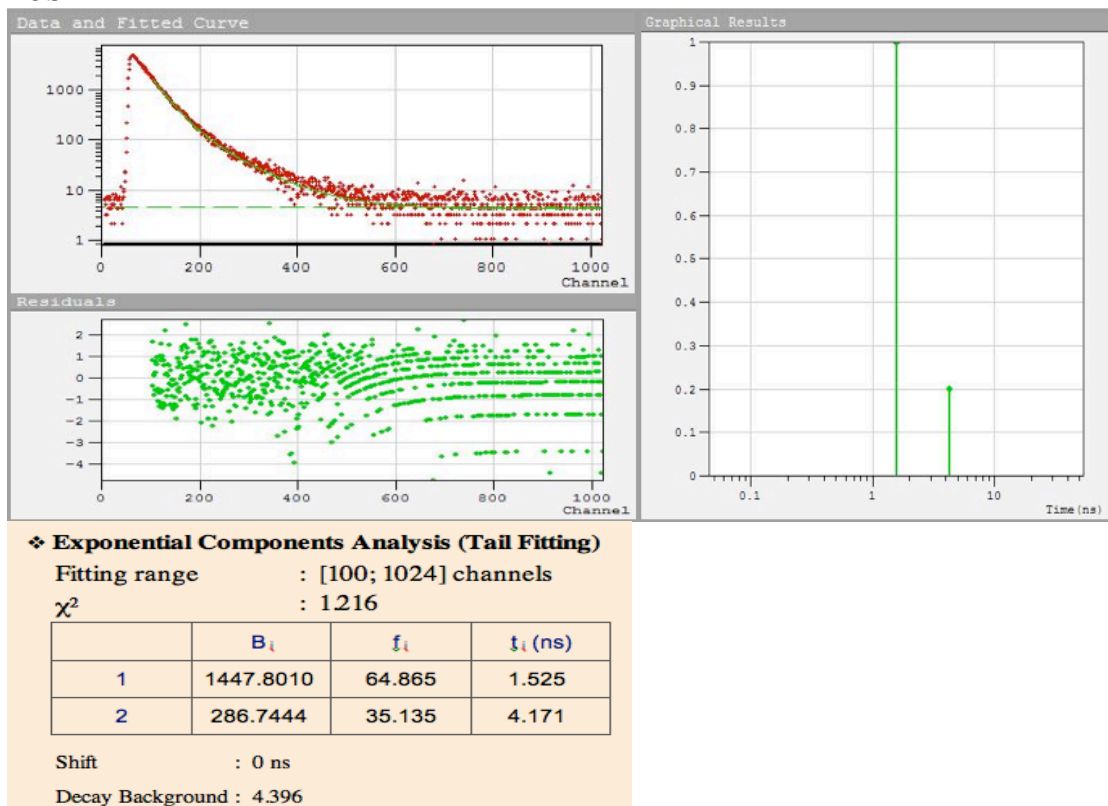
❖ Exponential Components Analysis (Tail Fitting)

Fitting range : [100; 1024] channels
 χ^2 : 1.201

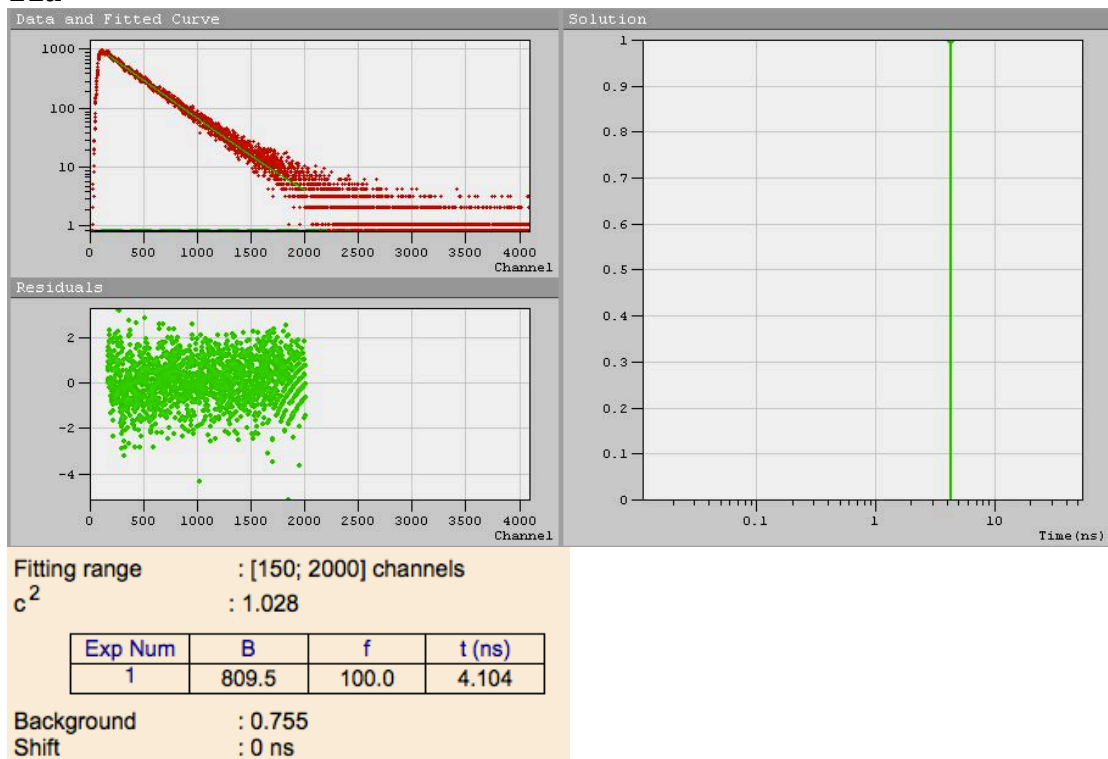
	B _i	f _i	t _i (ns)
1	88.5537	0.921	0.810
2	1855.0070	99.079	4.161

Shift : 0 ns

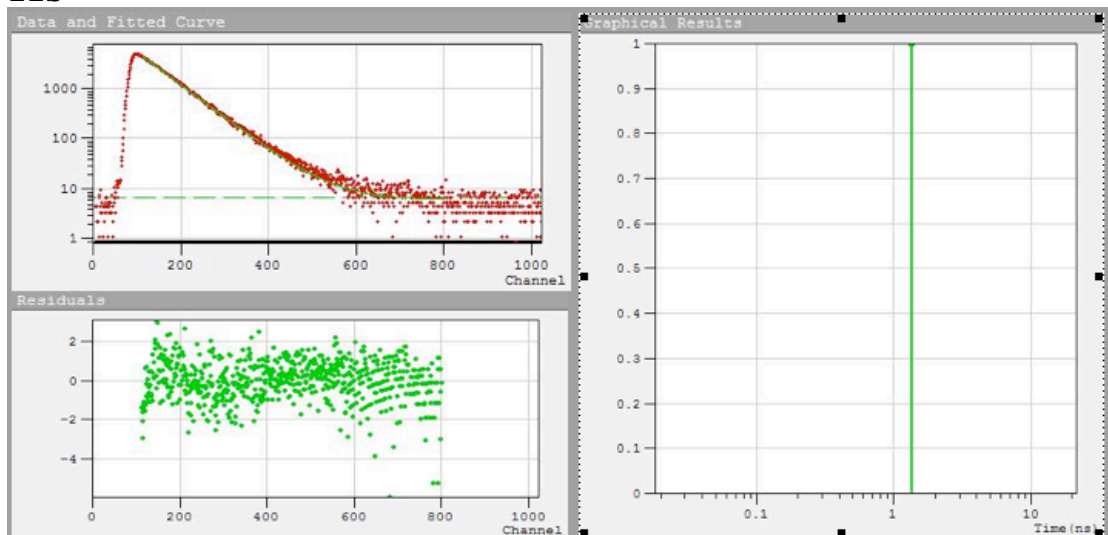
Decay Background : 5.529

10a**10b**

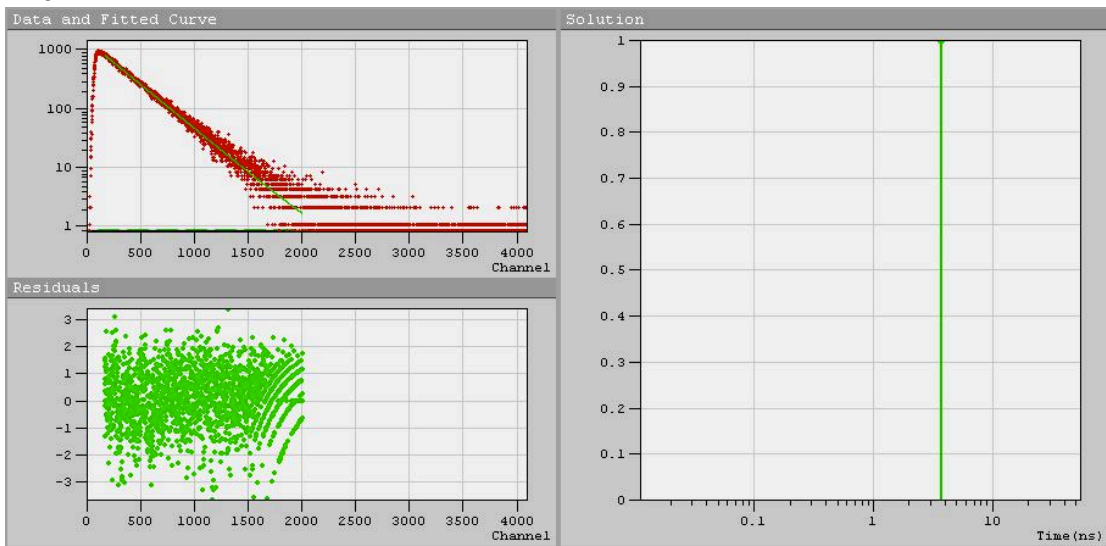
11a



11b



12a



v Discrete Components Analysis (Tail fitting)

Fitting range : [150; 2000] channels

c^2 : 1.062

Exp Num	B	f	t (ns)
1	807.2	100.0	3.568

Background : 0.210

Shift : 0 ns